Precursors to Atmospheric Blocking Events

by

Garrett P. Marino

B.S., Earth, Atmospheric, and Planetary Sciences (2008)
Massachusetts Institute of Technology

Submitted to the Department of Earth, Atmospheric, and Planetary Sciences
in Partial Fulfillment of the Requirements for the Degree of
Master of Science in Atmospheric Science

at the

Massachusetts Institute of Technology

June 2009

Signature of Author .....
Department of Earth, Atmospheric, and Planetary Sciences
June 1, 2009

Certified by .....
Lodovica C. Illari
Senior Lecturer, Department of Earth, Atmospheric, and Planetary Sciences
Thesis Supervisor

Accepted by .....
Maria T. Zuber
E.A. Griswold Professor of Geophysics
Head, Department of Earth, Atmospheric, and Planetary Sciences

Precursors to Atmospheric Blocking Events

by

Garrett P. Marino

Submitted to the Department of Earth, Atmospheric, and Planetary Sciences
on June 1, 2009 in Partial Fulfillment of the
Requirements for the Degree of Master of Science in
Atmospheric Science

ABSTRACT

Atmospheric blocking events disturb synoptic-scale features from their normal eastward progression, causing anomalous weather conditions for the duration of the blocking event. The essence of blocking can be captured by variation of potential temperature (θ_{trop}) on the dynamically-defined tropopause, considered as the 2 potential vorticity unit (PVU) surface. A climatology is constructed on winter ERA-40 data (DJFM 1957/58–2001/02) of θ_{trop} and wind. The climatology reveals a maximum in blocking activity over the eastern Atlantic.

Long-lasting (> 10 days) Atlantic sector (0–45°W) blocks are then identified using a blocking index developed by Pelly and Hoskins (2003), which detects reversals of the usual meridional θ_{trop} gradient. A composite of the 32 cases identified reveals that a blocking precursor signal, serving as an indicator of meridional flow preceding the onset of persistent Atlantic blocking episodes, can first be identified over the Pacific two weeks prior to genesis. The composite shows the precursor signal to be consistent with a transitioning positive-to-negative phase PNA, while the composite mature phase of Atlantic blocking resembles the negative phases of the NAO and AO. The results suggest that non-ephemeral blocking is a global, rather than localized, phenomenon.

Thesis Supervisor: Lodovica C. Illari
Title: Senior Lecturer, Department of Earth, Atmospheric, and Planetary Sciences

ACKNOWLEDGMENTS

The author wishes to express his gratitude to Dr. Lodovica Illari, who, as thesis supervisor, provided valuable guidance and assistance during this work's various stages of development. Special thanks to Professor Alan Plumb and Professor John Marshall for serving as members of the author's thesis committee and for providing feedback on this work. Thanks are also due to Dr. William Boos of Harvard University and David Stepaniak of the National Center for Atmospheric Research for their assistance in preparing some of the data used in this study.

CONTENTS

LIST OF FIGURES

LIST OF TABLES

1 Introduction

Atmospheric blocking is associated with vertically coherent, quasi-stationary high pressure "blocking" the normal westerly migration of weather systems. Blocking has been recognized for many decades as a significant component of atmospheric low-frequency variability. Rex (1950a,b) produced the first climatology of blocks, and also defined criteria for blocking. Rex identified a variety of anticyclonic blocking flows, in particular the Rex block named after the scientist. A Rex block (Fig. 1a) consists of a north-south orientated dipole with high pressure located poleward of low pressure, and occurs often over the northeastern Atlantic. Another type of blocking flow often discussed in the literature is the omega block (Fig. 1b), with streamlines resembling the Greek letter omega, commonly found over the Pacific. Note that both types involve quasi-stationary high pressure modifying the westerly flow.

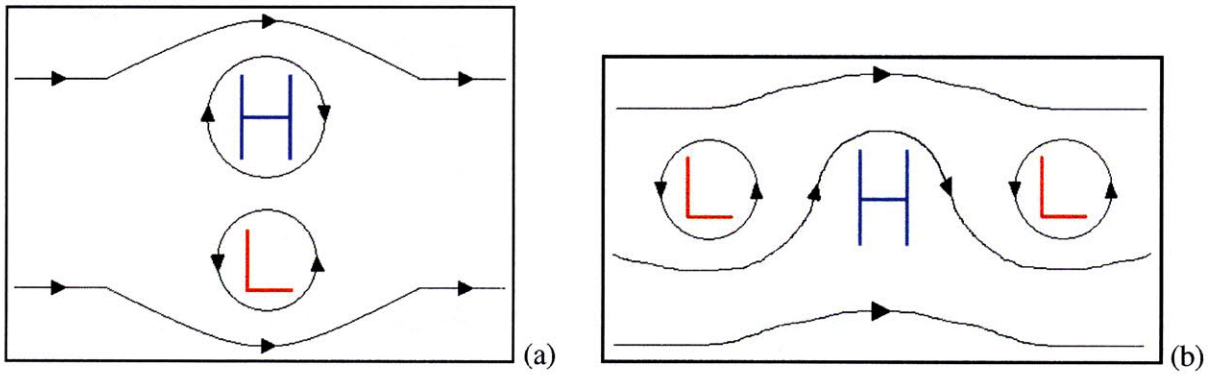

Figure 1: Schematic representations of (a) a Rex block and (b) an omega block. Areas of high (H) and low (L) pressure are indicated, along with streamlines corresponding to the direction of flow in the Northern Hemisphere.

Since the seminal work of Rex, may attempts have been made to objectively identify blocking events. Many researchers have used the Tibaldi and Molteni (1990) blocking index, which detects positive poleward gradients in the 500 hPa height field. The 500 hPa surface serves as a troposphere midpoint indicator for blocking. However, the blocking signal reaches

its peak higher in the atmosphere near the tropopause. Consequently, there has been a recent shift toward a dynamical potential vorticity (PV) framework for blocking (e.g., Pelly and Hoskins 2003, Croci-Maspoli et al. 2007a). The mandatory aspect of a block, a quasi-stationary anticyclone, can be thought of as a negative PV anomaly for the latitudes in which it resides. Furthermore, a constant PV surface can represent the dynamical tropopause. This PV framework will be used here to identify persistent blocking events and their precursors. (For more on the PV framework, see section 2.)

Theories explaining blocking onset can be categorized into two groups (Tyrlis and Hoskins 2008a), one that stresses the importance of *global* processes such as interaction of large-scale waves, and another detailing *local* processes such as strong cyclogenesis. The main aim of this work is to show that blocking is a global, rather than localized, phenomenon. A long-term climatology of the dynamical tropopause (section 3) is used in conjunction with the climatology of a dynamical blocking index (section 4) to confirm the results of other climatologies showing maxima in blocking frequency and duration over the eastern Atlantic region (e.g. Tyrlis and Hoskins 2008a). Precursors to persistent Atlantic blocking events are then explored in section 5. The precursor signal is connected to large-scale climate modes (teleconnections) in section 6. The discussion throughout is mostly through the behavior of composites of many events, but several case studies are also presented. Key findings and opportunities for further work are detailed in section 7.

2 PV Framework for Blocking — A Case Study

Until recently, many studies objectively identified blocks using a version of Tibaldi and Molteni's (1990) blocking index, which detects positive poleward gradients of the 500 hPa height field. An example of a high-low dipole Rex block detected by Tibaldi and Molteni's index is shown in Fig. 2.

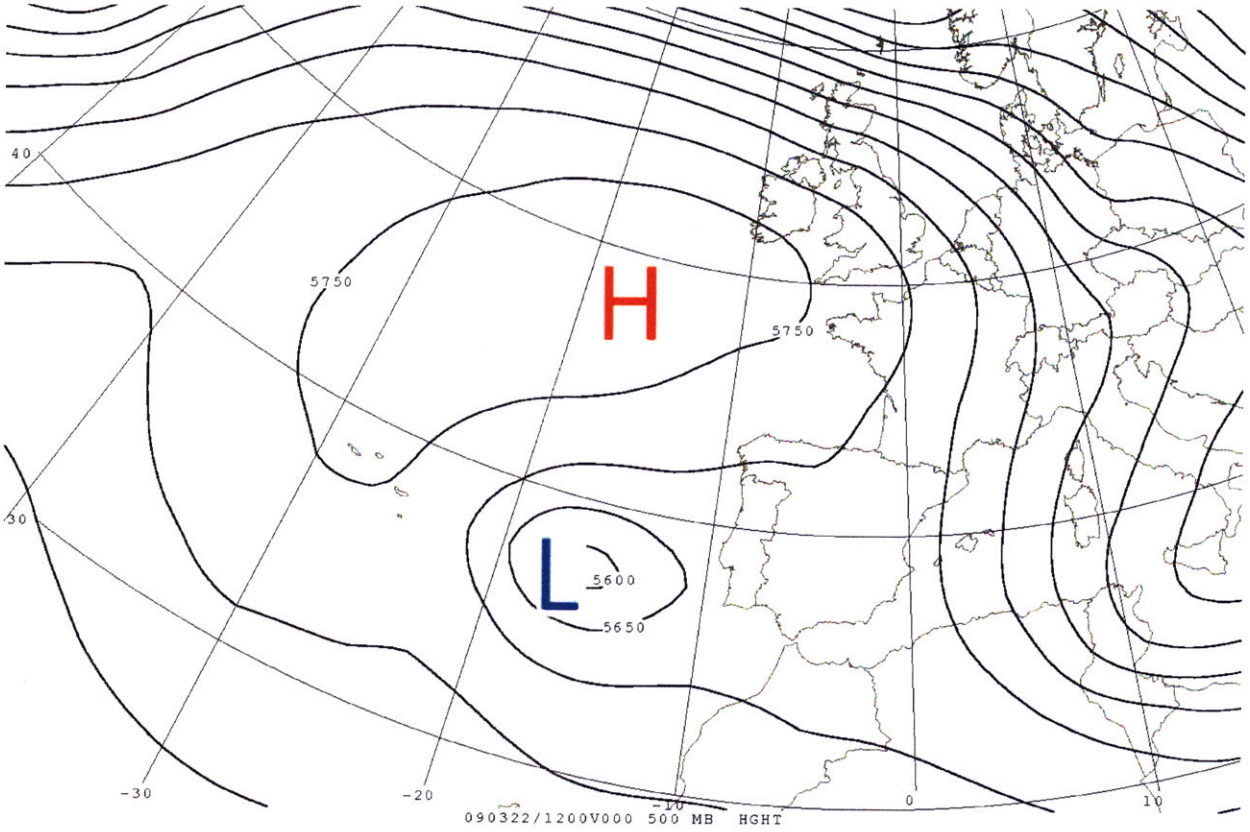

Figure 2: 500 hPa height over the eastern Atlantic on 12Z 22 March 2009, contoured every 50 m. A high(H)-low(L) dipole Rex block is clearly visible.

The 500 hPa height approach to block detection has limitations. This quantity is not conserved, while blocking has its maximum signature closer to the tropopause. The tropopause separates the troposphere from the highly stable stratosphere where isentropes are tightly packed. The literature commonly defines the tropopause dynamically as the 2 PV unit (PVU) surface

(1 PVU = 10^{-6} K kg^{-1} m^2 s^{-1}). Isentropic potential vorticity (q) is a conserved quantity sensitive to stratification:

$$q = -g\,(\zeta_\theta + f)\frac{\partial \theta}{\partial p}, \tag{1}$$

where ζ_θ is the relative vorticity on an isentropic surface, g is the acceleration due to gravity, f is the planetary vorticity, θ is potential temperature, and p is pressure. This quantity is conserved in adiabatic, frictionless flow. Since f is greatest at the pole, and the vertical gradient of θ increases dramatically near the tropopause, the climatological region of highest (lowest) PV in the troposphere resides on the polar tropopause (tropics).

The essence of blocking can be represented by this PV framework. As shown by Pelly and Hoskins (2003), blocking involves the breaking of upper-level Rossby waves on the dynamical tropopause, which leads to an isentropic meridional reversal of PV gradients (see, e.g., Hoskins et al. 1985 or Martius et al. 2008 for more on this). Persistent large-scale wave-breaking is a good indicator that blocking is occurring. The main premise is that subtropical air, with its low PV on a θ surface, is advected poleward by a strong cyclone. As the air moves poleward towards regions of typically higher PV, the advected airmass develops into a negative PV anomaly which results in an anticyclonic circulation. This high pressure region can then force upstream weather systems to stretch meridionally and continue advecting subtropical air into the block, extending the block's lifetime. Figs. 3 and 4 show meridional cross-sections of θ and PV for the Rex block case previously depicted in Fig. 2.

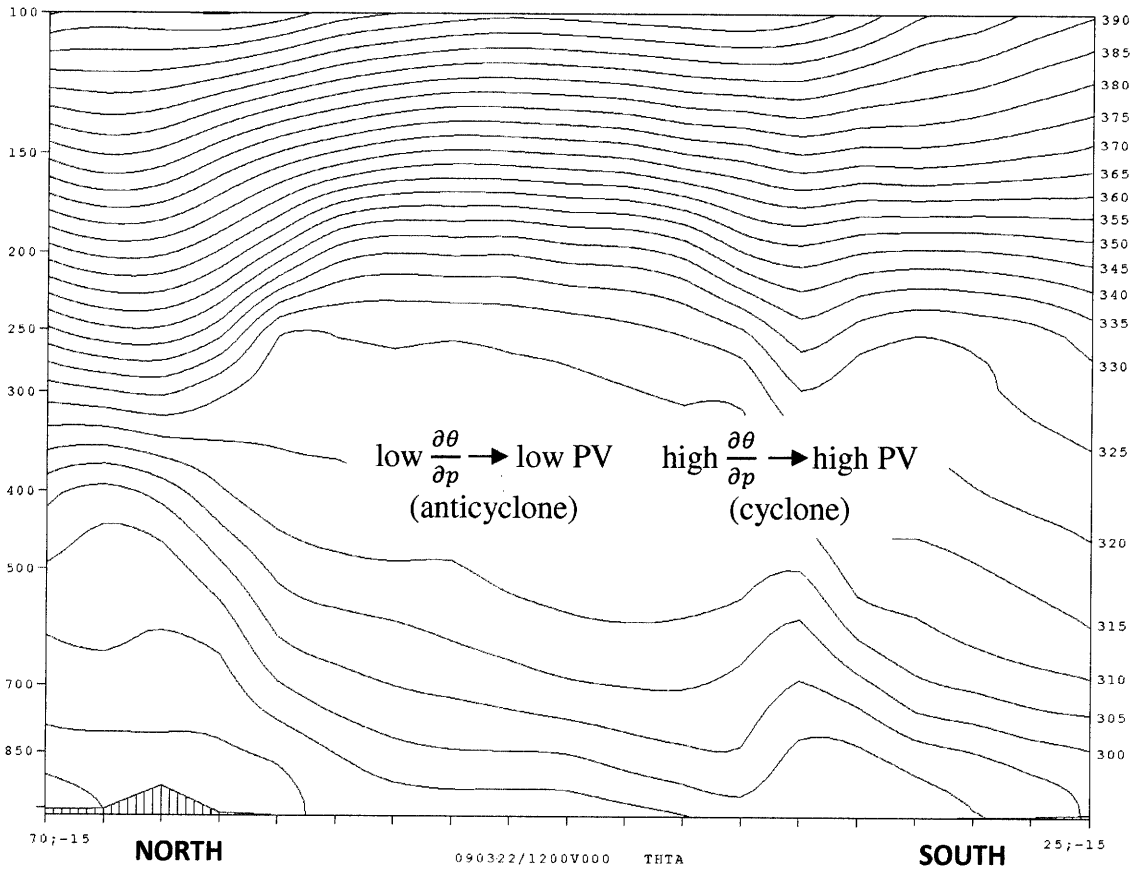

Figure 3: θ cross-section for the Rex block in Fig. 2 from 25-70°W along meridian 15°W, with pressure (in hPa) as the vertical coordinate. Contour interval is 5 K. The blocking anticyclone (cyclone) is associated with a region of low (high) vertical θ-gradients, indicating a region of anomalous low (high) PV. See Fig. 4 for the PV cross-section.

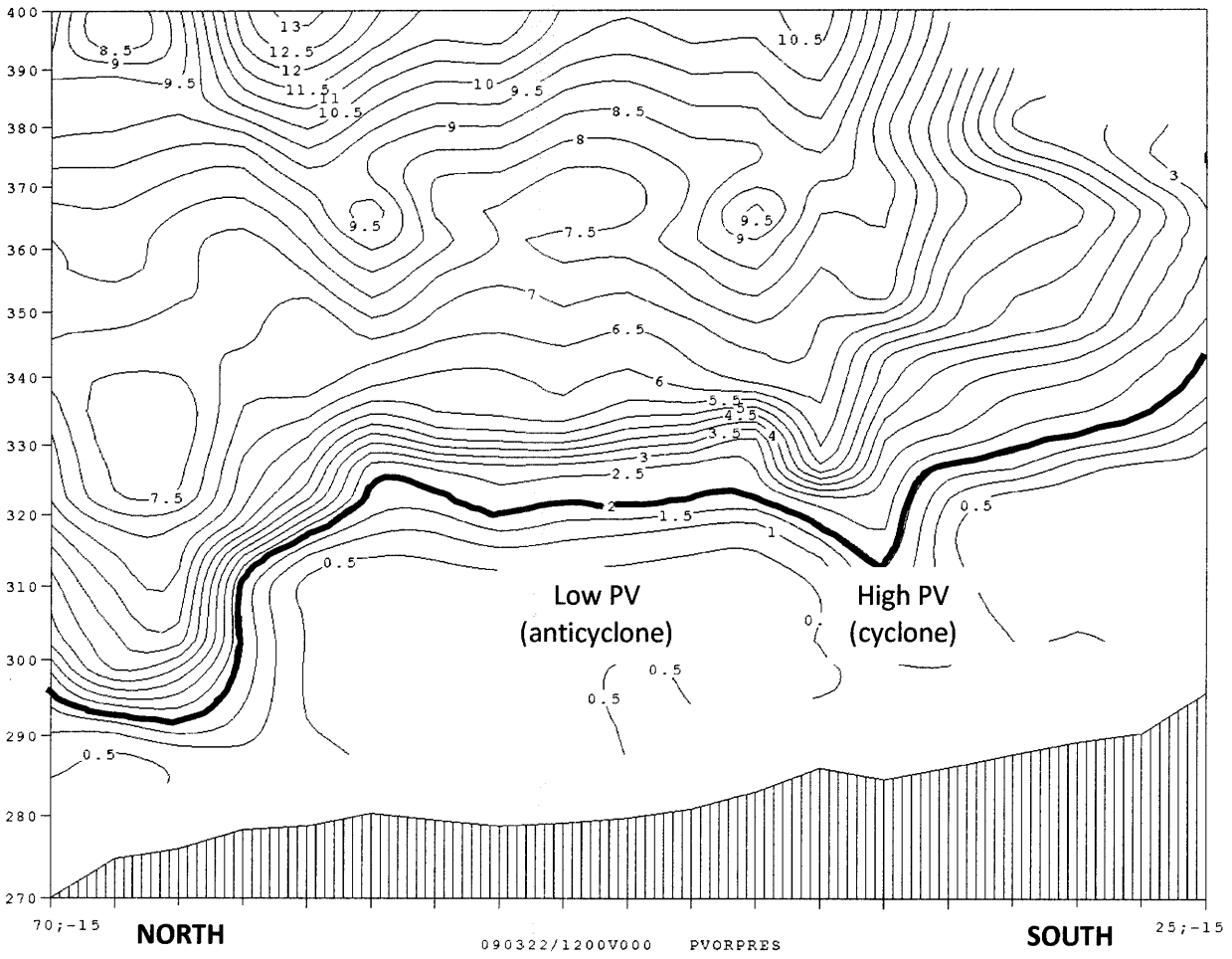

Figure 4: PV cross-section for the Rex block in Fig. 2 from 25-70°W along meridian 15°W, with θ as the vertical coordinate. Contour interval is 0.5 PVU. The bold line marks the tropopause (2 PVU surface). The blocking anticyclone (cyclone) is associated with a low (high) PV airmass, with corresponding high (low) tropopause θ. Compare to the tropopause θ climatology in Fig. 6b.

To identify blocks and their precursors, one can consider the advection of potential temperature on the tropopause. The tropopause can be computed on different isentropic surfaces (see Fig. 5), and a composite of these horizontal maps will illustrate the height of the tropopause (given by θ) over a large region. The composite maps can then be used for block detection.

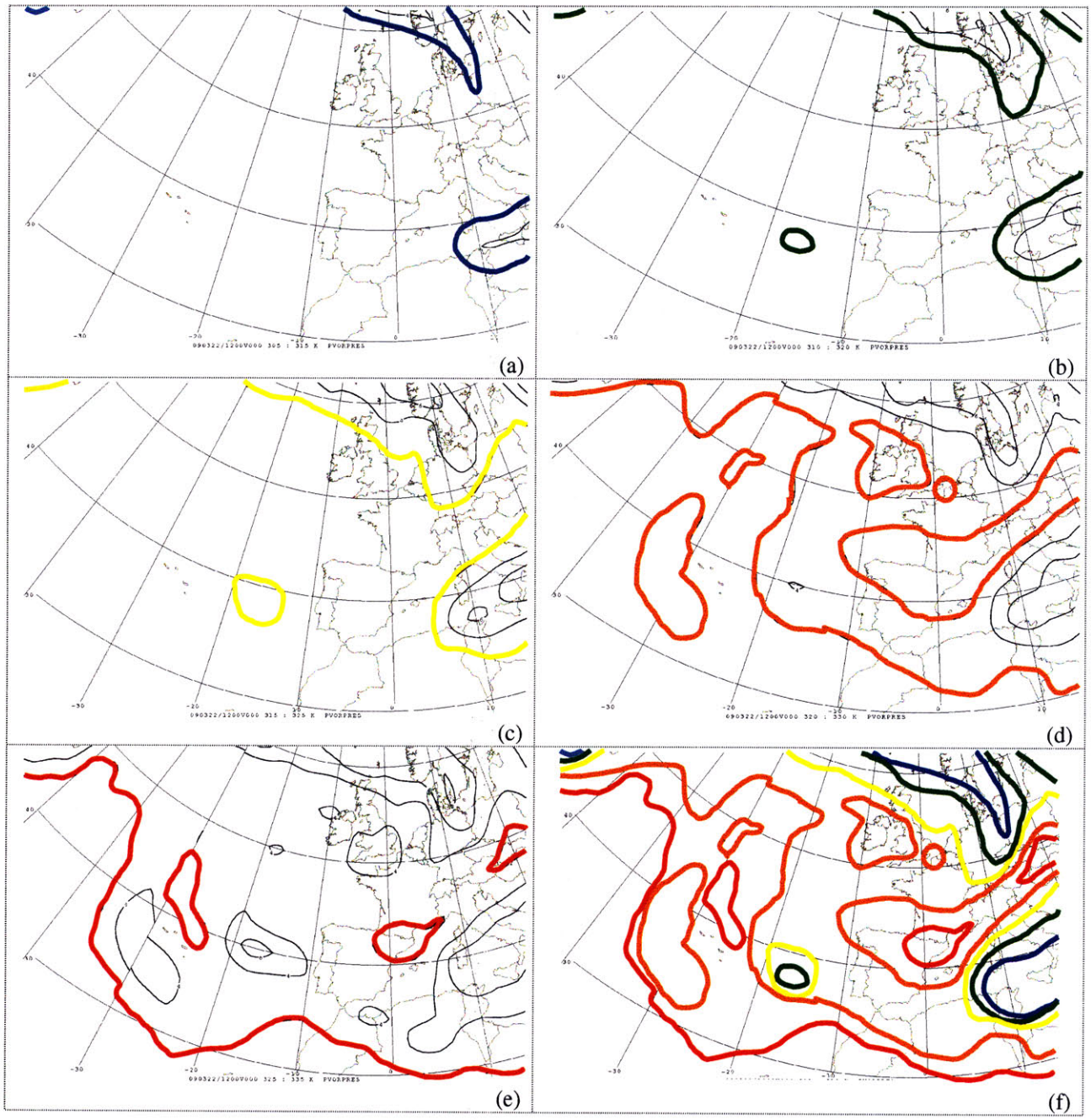

Figure 5: Potential vorticity on various isentropic surfaces for the Rex block in Fig. 2, contoured every 2 PVU. The 2 PVU surface is highlighted on the (a) 310 K, (b) 315 K, (c) 320 K, (d) 325 K, and (e) 330 K isentropic surfaces. A composite of the 5 maps is given in (f), clearly showing warm (high) tropopause to the north in the blocking anticyclone and cold (low) tropopause to the south in the cyclone.

3 Climatology of the Dynamical Tropopause

Production of a long-term climatology of tropopause θ (θ_{trop}) and wind has been computed using the ERA-40 reanalysis of the ECMWF (Uppala et al. 2005) for the time period December 1957 to March 2002, available through NCAR (NCAR). Northern Hemisphere winter (DJFM) potential temperature and zonal and meridional winds on the 2 PVU surface were extracted from the ds117.4 dataset, "ERA-40 model resolution gridded upper air analysis on a potential vorticity surface." The dataset's full temporal resolution of 6 hours was used and the original fields were interpolated from a reduced n80 Gaussian grid to a regular 2.5° × 2.5° grid at NCAR. These GRIB1 files were then converted to binary files and read into MATLAB for analysis.

The main diagnostic blocking variable employed here is θ_{trop}, serving as an indicator of tropopause height. The ERA-40 climatology of this variable during winter is shown in Fig. 6. Note the high tropopause over the tropics (where the surface is also warmest) and low tropopause over the pole.

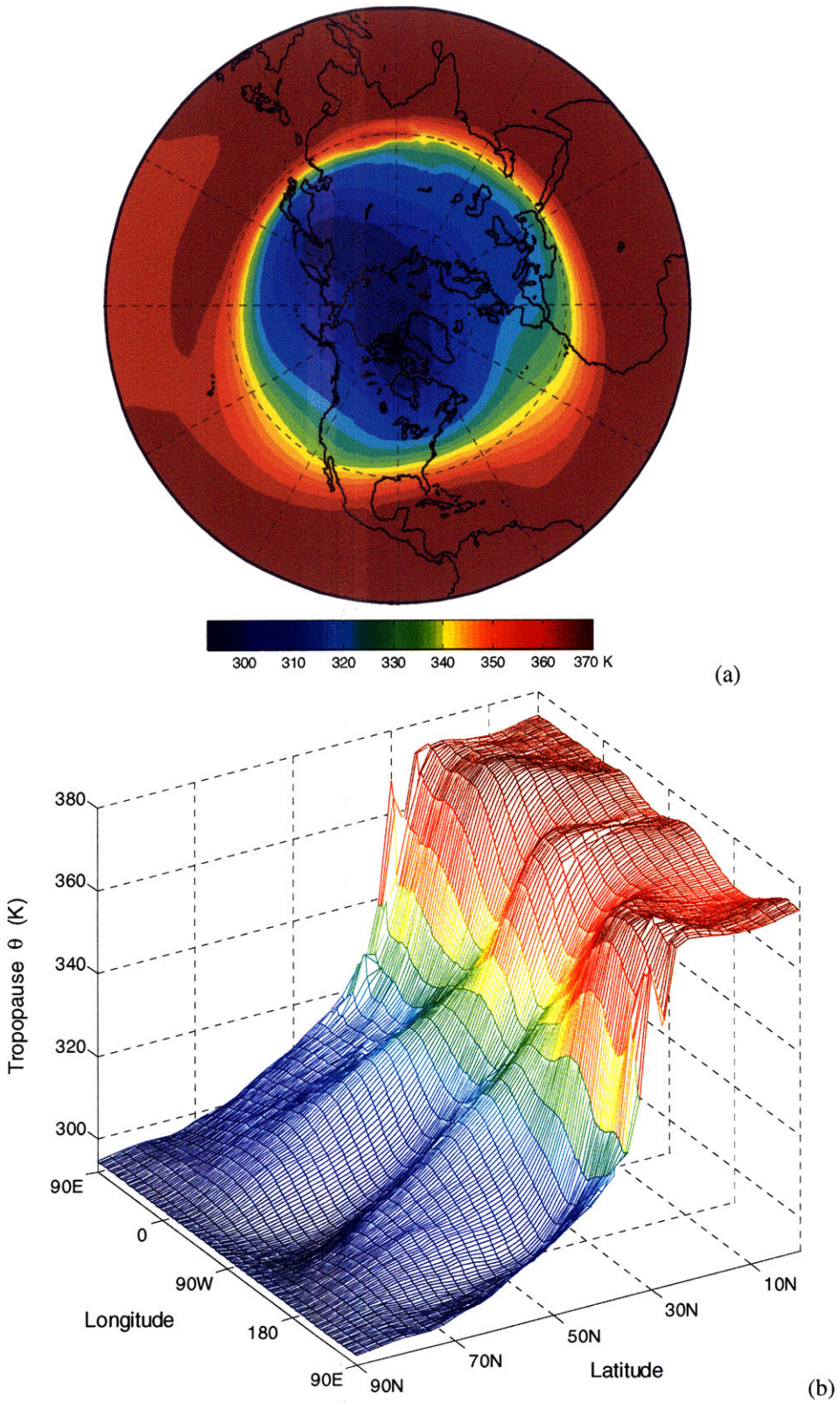

Figure 6: θ_{trop} climatology during winter (DJFM 1957/58 – 2001/02). Shading contour is 5 K. θ_{trop} is the vertical coordinate in (b), depicting the height of the tropopause. Note its sharp downward slope over the midlatitudes, and the presense of standing waves on this surface with troughs over land and ridges at the end of the Pacific and Atlantic storm tracks.

The θ_{trop} climatology in Fig. 6 reveals some well-known aspects of the general circulation. Standing waves are clearly visible, with troughs over the cold landmasses during winter and ridges over the relatively warm ocean basins. Divergent flow is observed over the end of both the Pacific and Atlantic storm tracks, where the jet is fairly weak (see Figs. 7-8). The regions of divergent flow might correspond to maxima in blocking activity, since blocking acts to redistribute meridional θ_{trop} gradients. Taking the difference in climatological θ_{trop} between the parellels capturing the storm track and largest θ_{trop} gradient, 20°N and 60°N (Fig. 9), local minima are found over the eastern Pacific and eastern Atlantic regions, suggesting maxima in blocking activity over these regions. The next section describes an index used to objectively identify blocking events and check this result.

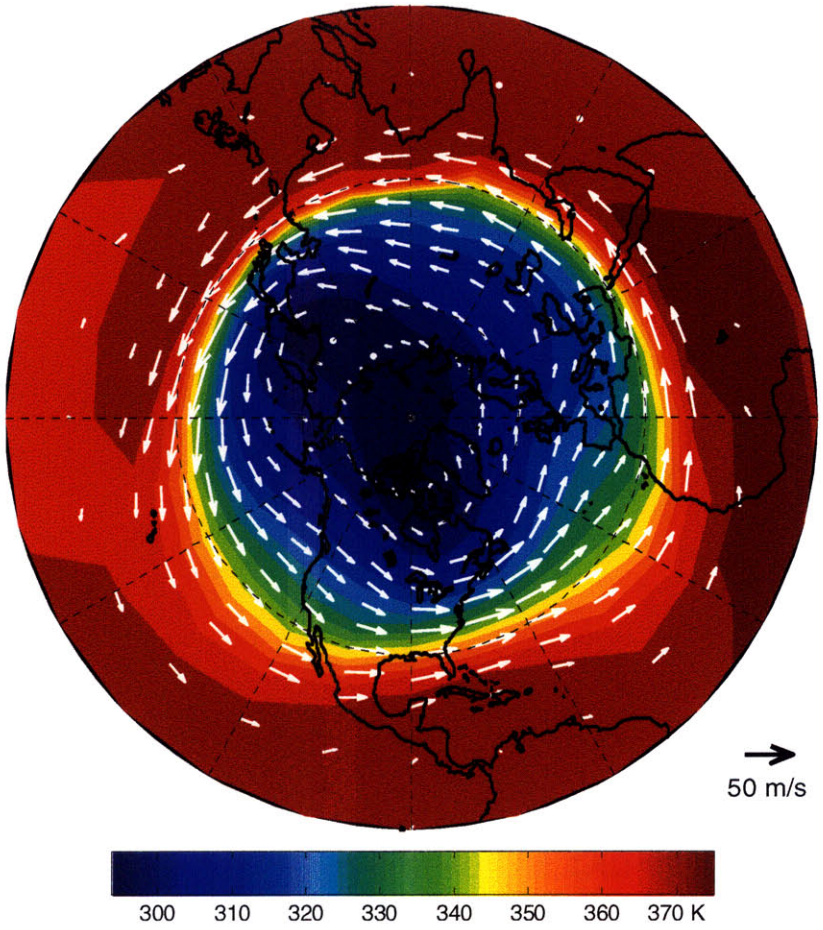

Figure 7: Same as Fig. 6, now with climatological wind vectors showing that the wind follows the θ contours and that the strongest winds are located in regions of largest meridional θ gradient.

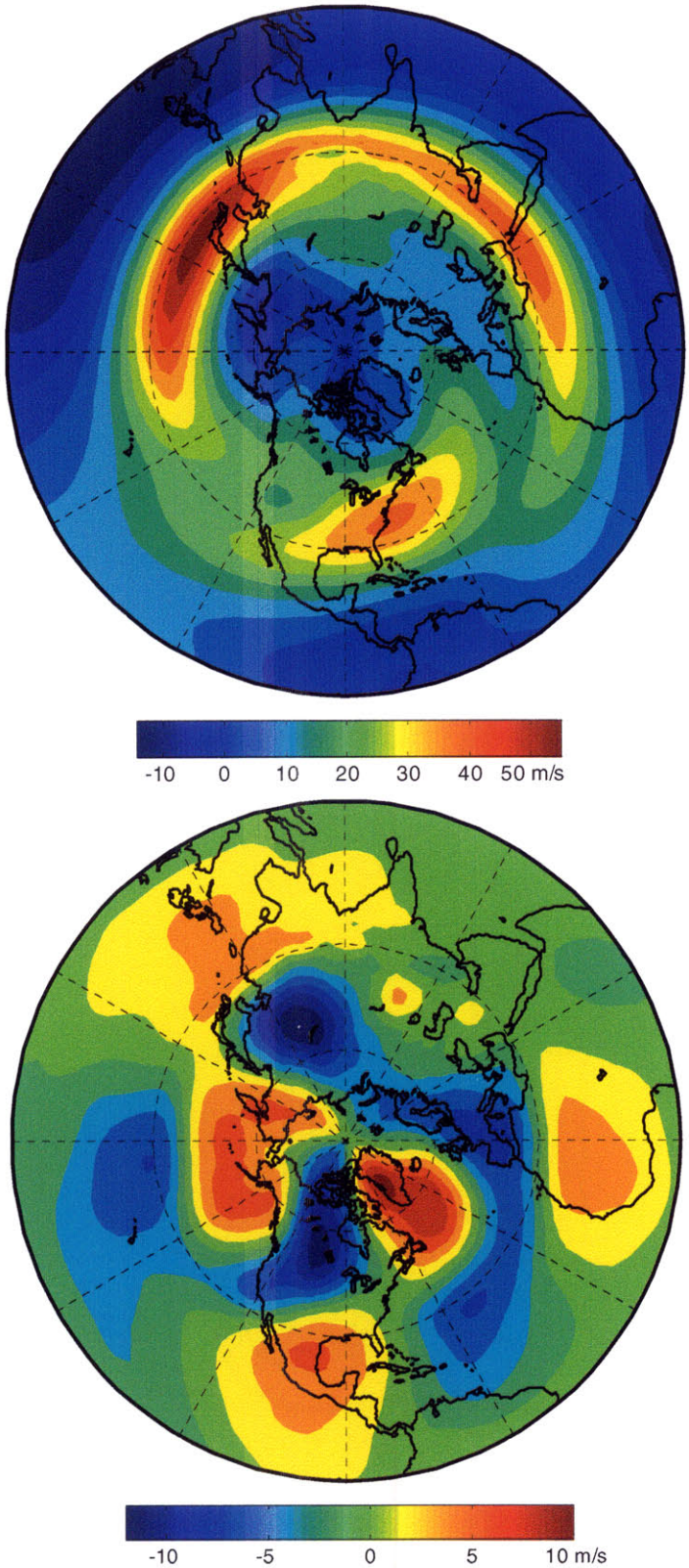

Figure 8: Climatological wind on the tropopause during winter (DJFM 1957/58 – 2001/02): (a) zonal component, contour interval 5 ms^{-1}, and (b) meridional component, contour interval 2 ms^{-1}. Note the northerly meridional flow over the cold landmasses and southerly flow over the northern oceans.

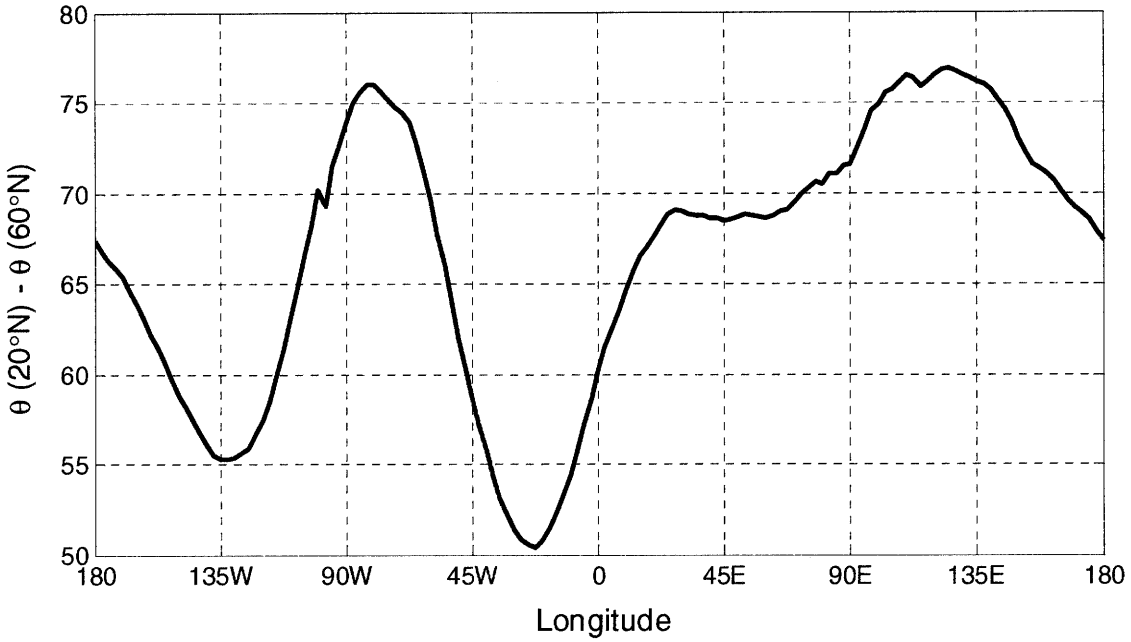

Figure 9: Climatological difference in θ_{trop} between 20°N and 60°N (DJFM 1957/58 – 2001/02). Note the minimum near 22.5°W, suggesting a maximum of blocking action over the eastern Atlantic region.

These climatological results are consistent with a long-term climatology published recently by Tyrlis and Hoskins (2008a,b).

4 Dynamical Blocking Index

To objectively define blocking events and thus build a blocking climatology, the index of Pelly and Hoskins (2003) is employed, which detects blocks as reversals in the usual meridional θ_{trop} gradient. Fig. 10 illustrates a θ_{trop} field exhibiting two blocks. In the example, subtropical air (with its warm tropopause) has been advected far north over both Alaska and the eastern Atlantic. The anomalous airmasses are both about to cut off from their regions of origin, and can only disappear through diabatic processes, friction, or if they return back south.

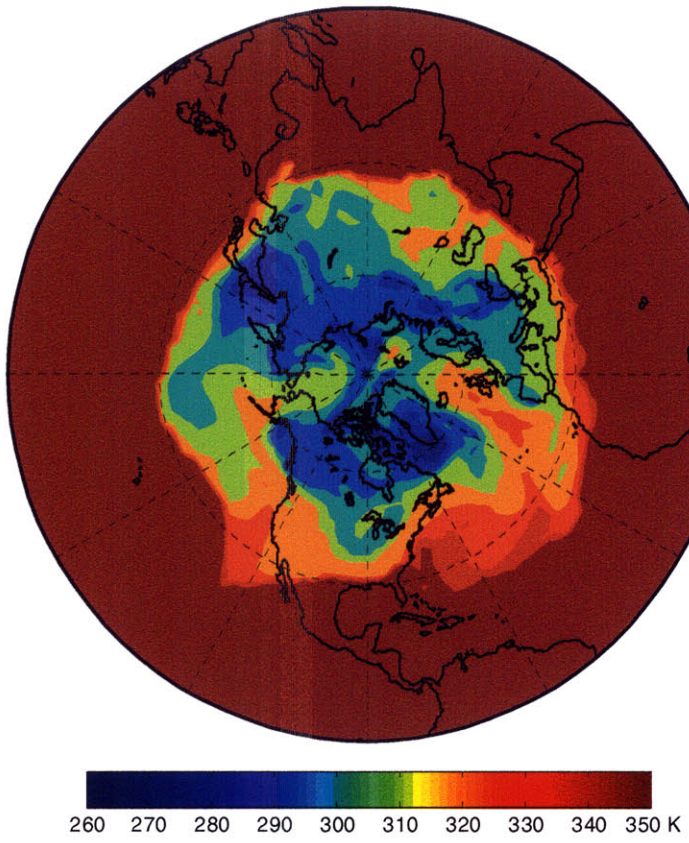

Figure 10: Instantaneous θ_{trop} for 12Z 19 February 1992, contoured every 10 K. Note the blocks over the eastern Atlantic and Alaskan regions during this time.

The blocking pattern can be represented schematically as in Fig. 11, showing an intrusion of warm tropopause to the north and accompanying cold tropopause to the south. Pelly and Hoskins defined the central blocking latitude (ϕ_0) of their index as a function of longitude (λ), based on the maxima of the climatological 300 hPa high-pass transient eddy kinetic energy during winter (DJF). θ_{trop} is then averaged at each longitude over the regions 0-15° north and 0-15° south of this central blocking latitude. Pelly and Hoskins also average θ_{trop} over 5° longitudinal strips, but here simply an average of a one-dimensional meridional cross-section is considered. The central blocking latitude is also allowed to vary by 5°, similar to Pelly and Hoskins. The blocking index (B) is then defined as the maximum value of the difference between the θ_{trop} averages north and south of the central blocking latitude, with $B > 0\,\mathrm{K}$ indicating a block at longitude λ:

$$B\,(\lambda) = \frac{2}{\Delta\phi}\left(\int_{\phi_0}^{\phi_0+\frac{\Delta\phi}{2}} \theta_{trop}(\phi,\lambda)\,d\phi - \int_{\phi_0-\frac{\Delta\phi}{2}}^{\phi_0} \theta_{trop}(\phi,\lambda)\,d\phi\right). \qquad (2)$$

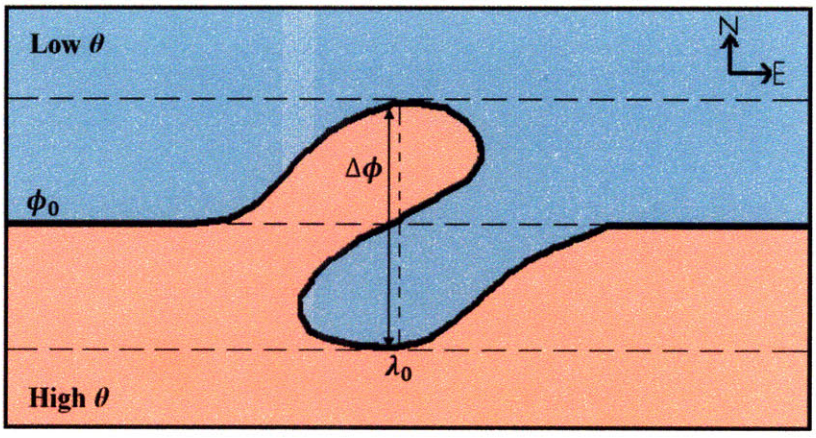

Figure 11: Schematic of the parameters used to compute the Pelly and Hoskins instantaneous blocking index at longitude λ_0. The thick black line is an isentrope, while the central blocking latitude is given by ϕ_0. $\Delta\phi$ is fixed at 30°. In this case, B >> 0. The perspective is from the Northern Hemisphere. (Modified from Pelly and Hoskins (2003).)

For the case shown in Fig. 10, the Pelly and Hoskins index captures the blocks over Alaska and the eastern Atlantic (Fig. 12).

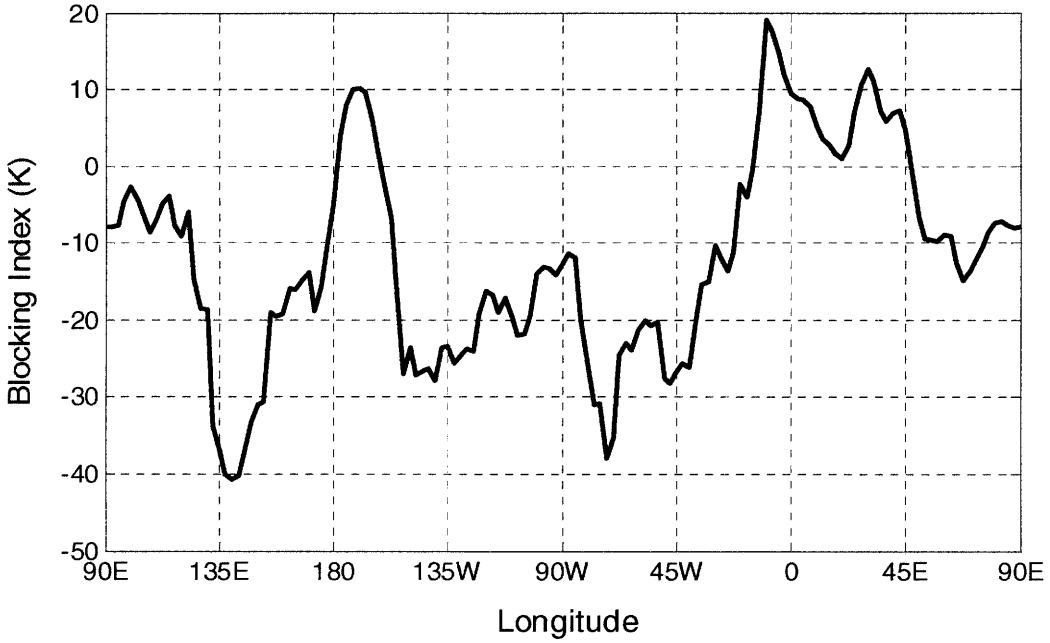

Figure 12: The Pelly and Hoskins index detects blocks over Alaska and the eastern Atlantic for the example shown in Fig. 10.

A 45-year blocking climatology using the same index (Fig. 13) reveals the highest blocking frequency of occurrence over the Euro-Atlantic sector, in agreement with Pelly and Hoskins' five-year climatology (2003) and a recent climatology using the ERA-40 database (Tyrlis and Hoskins 2008a). However, the Euro-Atlantic sector is already close to being blocked on average (Fig. 14). The average index value over this region is only slightly below zero. Tyrlis and Hoskins (2008a) recognized this, and upon also considering additional blocking criteria including temporal persistence and extensive aerial coverage, they still found a peak in blocking activity over the northeastern Atlantic. Furthermore, as will be discussed later in section 6, blocking over the Atlantic is almost always associated with the NAO- phase, and points commonly used to define the NAO index (Iceland and Azores) reside over the eastern Atlantic.

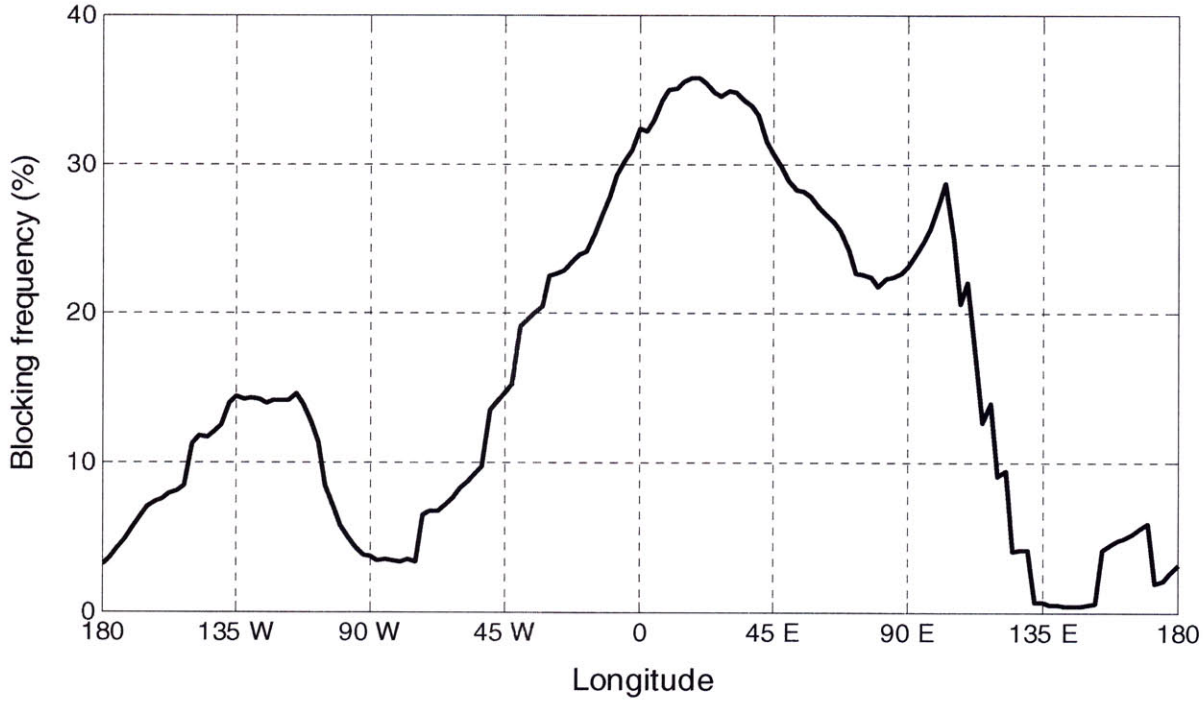

Figure 13: Local instantaneous blocking frequency of occurrence using the Pelly and Hoskins blocking index (DJFM 1957/58–2001/02). The climatology suggests that blocking flows tend to develop most often over the Euro-Atlantic region.

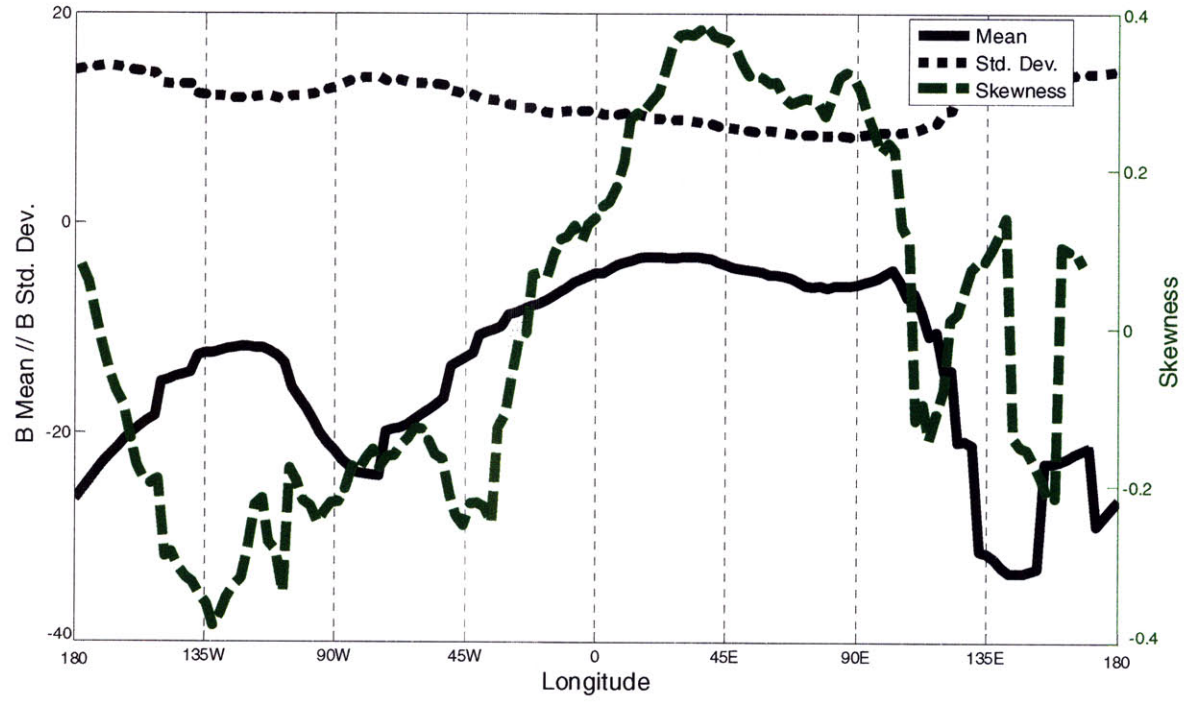

Figure 14: Longitudinal variation of the blocking index mean (solid line), its standard deviation (dotted black line), and skewness (green dashed line). Note that the European region is closest to being blocked (highest *B* mean). [Following Tyrlis and Hoskins 2008a, Fig. 4b.]

5 Precursors to Persistent Atlantic Blocking Events

5.1 Cases

The eastern Atlantic experiences the most frequent long-lived blocking events, thus the region is of great interest for exploring blocking precursors. These persistent blocks can span a great meridional extent, and could have their origins far upstream of where they mature. Upon considering the climatological minimum in the midlatitude meridional gradient of θ_{trop} (reflecting regions of blocking maxima) occurring near longitude 22.5°W (Fig. 9 above), the eastern Atlantic sector is defined here to span the region 0°–45°W. A similar longitudinal extent for sector blocking analyses has been employed throughout the literature (e.g., Rex 1950a,b, Tyrlis and Hoskins 2008b). The 45° extent exceeds what should be considered a minimum width of blocking, the Rossby radius of deformation, and also allows for slight movement of the block in the sector.

Persistent Atlantic sector blocking events are detected by averaging the Pelly and Hoskins index over meridians 0°–45°W during winter (DJFM) for the 45 years of the ERA-40 dataset. The average index value for every 6 hours is then averaged for 10-day periods, and a persistent event is detected if the10-day average exceeds zero. Blocking genesis (lysis) is defined as the beginning (end) of the first (last) 10-day nonnegative period. See Table 1 for dates of the 32 events detected over the period of record 1957–2002.

Table 1: Identified Atlantic Block Events

Case Number	Blocked Period	Block Duration (Days)
1	January 6 – 18, 1960	13
2	March 4 – 16, 1960	13
3	December 14 – 26, 1961	13
4	February 18 – March 5, 1962	16
5	December 21, 1962 – February 9, 1963	51
6	December 1 – 21, 1963	21
7	January 6 – March 18, 1964	73
8	January 24 – March 10, 1965	46
9	January 1 – 17, 1967	17
10	February 3 – March 16, 1968	43
11	December 18, 1970 – January 3, 1971	17
12	December 24, 1971 – January 11, 1972	19
13	March 6 – 28, 1972	19
14	January 1 – 11, 1973	11
15	February 1 – 13, 1975	13
16	December 1 – 23, 1975	23
17	December 14 – 27, 1976	14
18	December 16, 1978 – January 23, 1979	39
19	March 11 – 24, 1979	14
20	March 14 – 26, 1980	13
21	February 3 – 23, 1983	21
22	March 8 – 21, 1984	14
23	January 29 – February 10, 1986	13
24	January 19 – February 2, 1987	15
25	December 1 – 10, 1989	10
26	December 1 – 14, 1990	14
27	February 22 – March 11, 1993	18
28	December 4, 1995 – March 31, 1996	119
29	December 25, 1996 – January 10, 1997	17
30	December 12 – 26, 1997	15
31	January 9 – 29, 2000	21
32	December 8 – 24, 2001	17

Table 1 reveals two immediate observations on the detected Atlantic blocking events: (1) the least ephemeral and greatest number of events occur during the middle of winter (Fig. 15), suggesting that large-scale processes may have considerable influence on persistent

blocking events, and (2) a trend toward less frequent events over the period of record will be explored further in section 6.

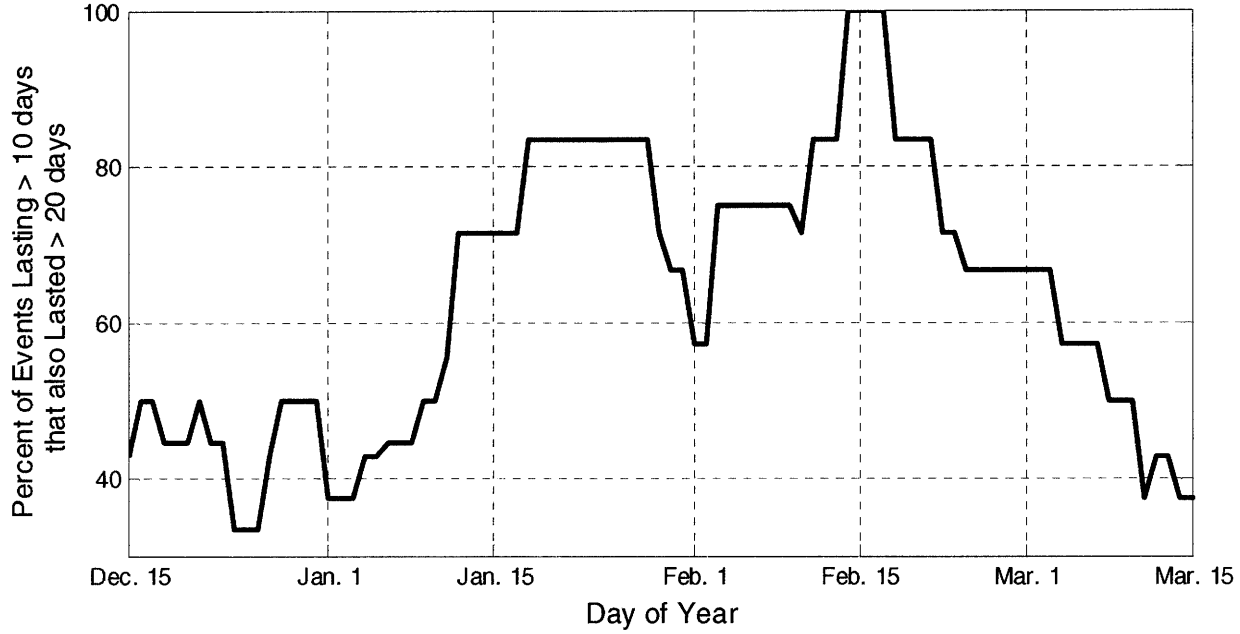

Figure 15: The percentage of identified Atlantic blocking events (10 day minimum) that also persist for over 20 days reaches a maximum during the middle of winter.

5.2 Composites

Anomalies of θ_{trop}, and tropopause zonal (U_{trop}) and meridional wind (V_{trop}), associated with each case are computed using the DJFM mean, but nearly identical patterns would result from a time-varying climatology. The tropopause composite during the mature Atlantic block stage (Fig. 16) clearly reveals the block's influence. The block modifies the westerly Atlantic jet, splitting it in two branches and replacing the region between the two with easterlies. The θ_{trop} and U_{trop} anomalies look similar because the zonal component of the wind is typically much greater than its meridional counterpart, and serves to advect warm or cold tropopause.

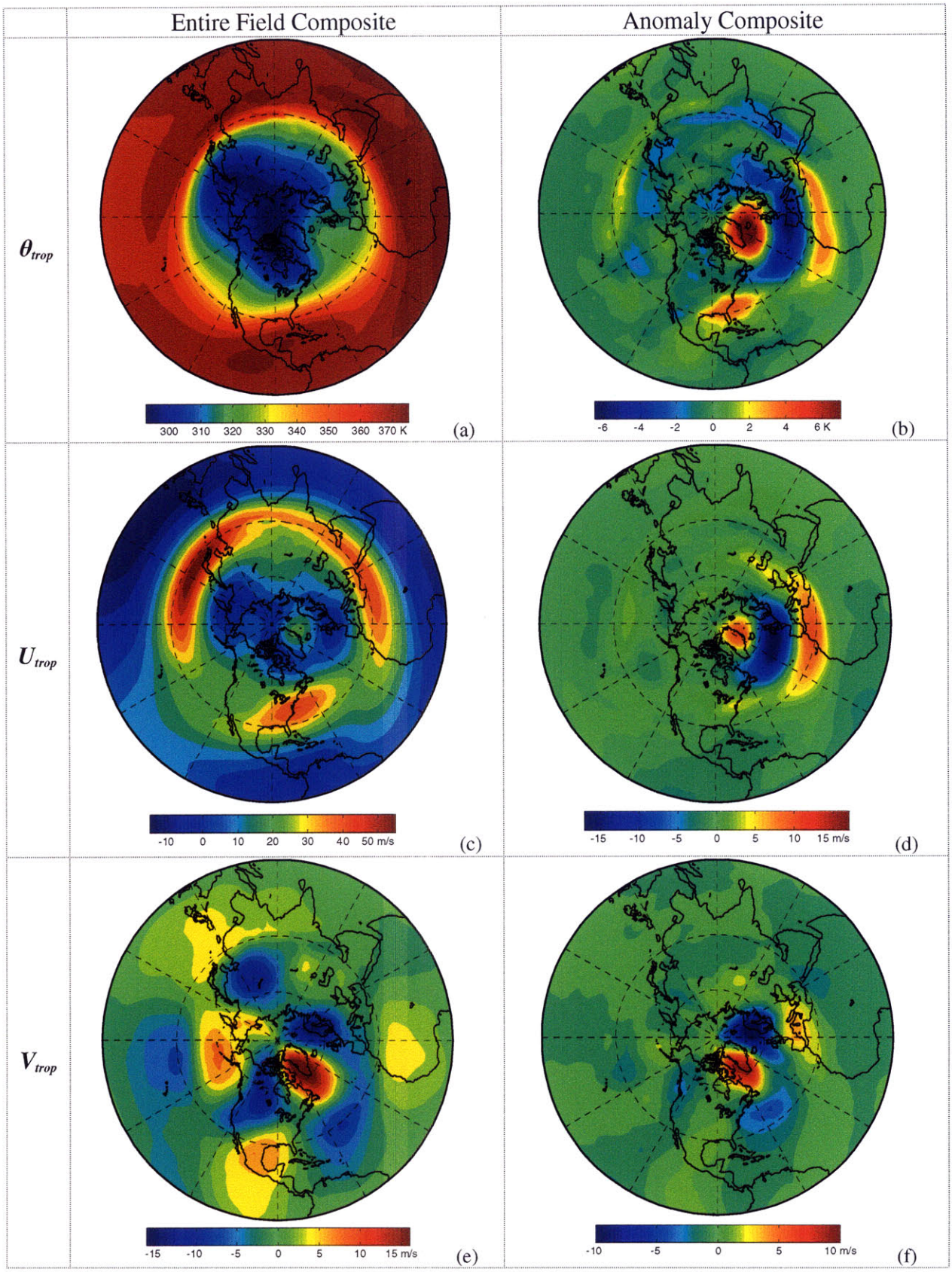

Figure 16: Composites for the mature phase of Atlantic blocking events: (a) θ_{trop}, (c) U_{trop}, and (e) V_{trop}, and their anomalies (b, d, f).

Tracing the evolution of 5-day average composite anomalies prior to Atlantic blocking reveals a precursor signal over the Pacific (Fig. 17). About 1-3 weeks prior to block onset, warm tropopause advects across the Pacific and the interaction with an enhanced Aleutian low expands the climatological geopotential ridge at the end of the storm track, establishing a meridional wave-train of anomalies across North America and into the western Atlantic. This stage of the precursor signal resembles the PNA+ phase, as discussed further in section 6. The cold tropopause over the southeastern United States eventually weakens and merges with a cold anomaly over the south-central Atlantic about a week prior to block onset. The anomalies over the Pacific are then allowed to migrate eastward over the United States, with a trough developing over the western part of the country. The cold tropopause then aids in the formation of a cyclone downstream over the southeastern United States days prior to block onset. Meanwhile, the south-central Atlantic cold anomaly and enhanced ridging over Europe are conducive to slow the movement of the cyclone, and act to stretch it meridionally, establishing the block. For the full time evolution (1-day resolution) of each variable, see the Appendix.

An example case study (Fig. 18) also shows a similar time progression to the composite presented in Fig. 17. In this case, a strong Pacific jet and enhanced Aleutian low act to advect warm tropopause over the end of the Pacific storm track. The warm anomaly eventually travels across North America, is further fed by synoptic development from the cold tropopause behind it, and interacts with a block over Europe to establish the Atlantic block.

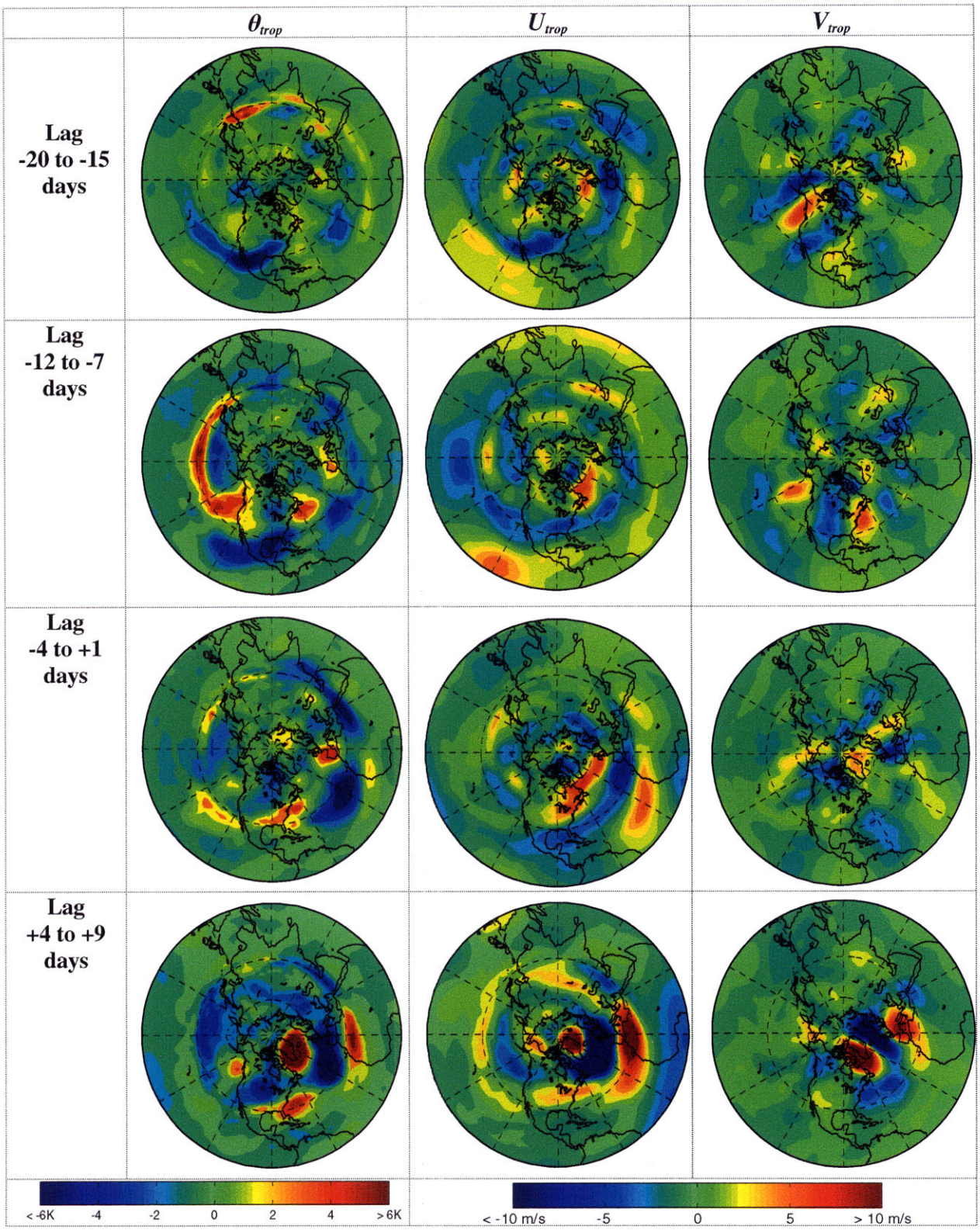

Figure 17: 5-day average composites of θ_{trop}, U_{trop}, and V_{trop} prior to and during Atlantic block onset. The θ_{trop} anomalies track well the Pacific precursor signal to three weeks prior to block onset. (For the full evolution of each variable, see the Appendix.)

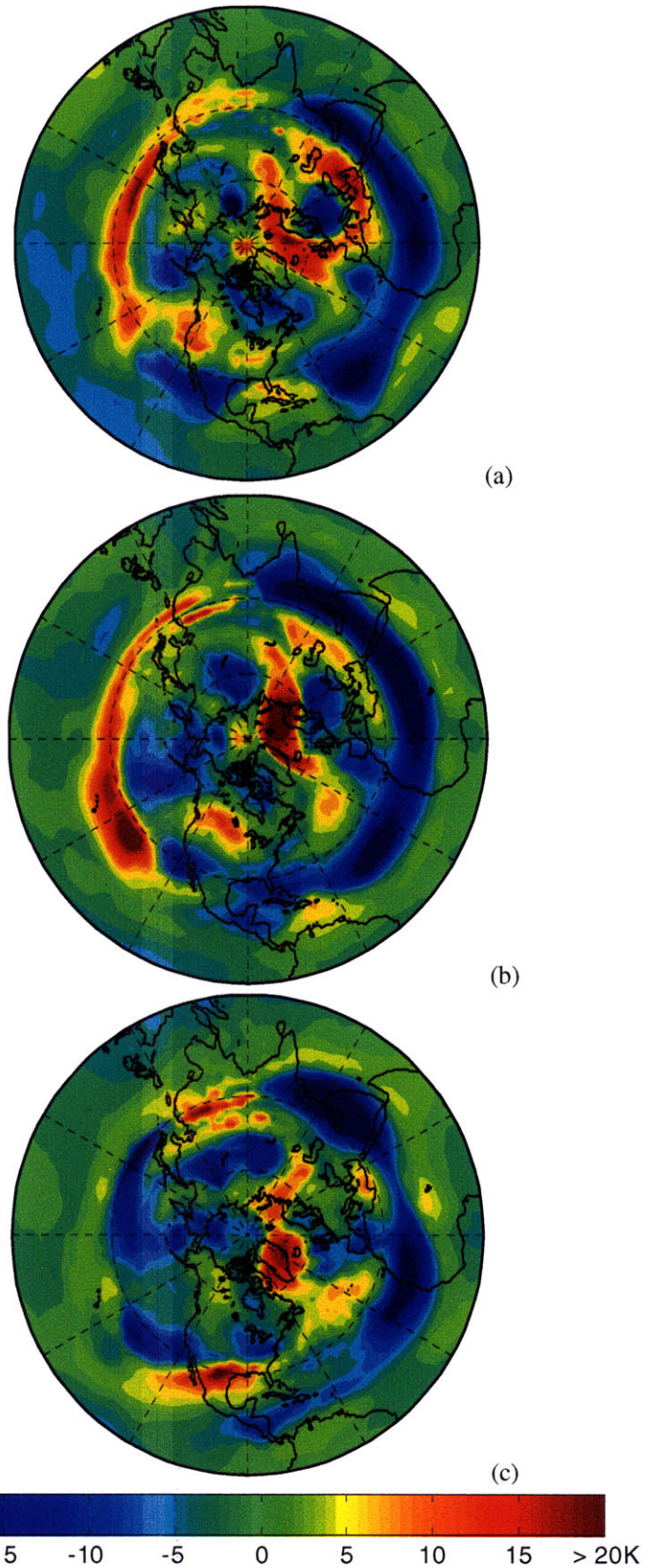

Figure 18: 5-day average θ_{trop} anomalies for the Atlantic blocking case during March 1979: (a) 5–10 days prior to block onset, (b) 0–5 days prior to onset, and (c) 5–10 days after block onset.

5.3 Hovmöller Diagrams of Blocking Precursors

As shown in the previous section, the precursor signal to the Atlantic blocking pattern originates in the Pacific as a pool of warm tropopause that eventually advects over to the Atlantic. Hovmöller diagrams are useful to show the progression of this global precursor signal.

As shown by the composite images above, the precursor signal originates in the subtropics, while the mature Atlantic block resides about 20–30° latitude farther north. Considering this for the Hovmöller diagram construction, the central blocking latitude of the Pelly and Hoskins index is allowed to be anywhere from 30°N–55°N at every longitude. This way, anomalies in the 'modified' index will capture the warm tropopause transport from the Pacific over to the Atlantic (Fig. 19).

To highlight the warm tropopause transport over the subtropics, a second Hovmöller diagram has been constructed of θ_{trop} anomalies averaged between about 30°N–40°N (Fig. 20). The diagram also clearly shows the warm anomaly associated with a strong cyclogenesis event over the southeastern United States, which is believed to be a vital factor in blocking onset.

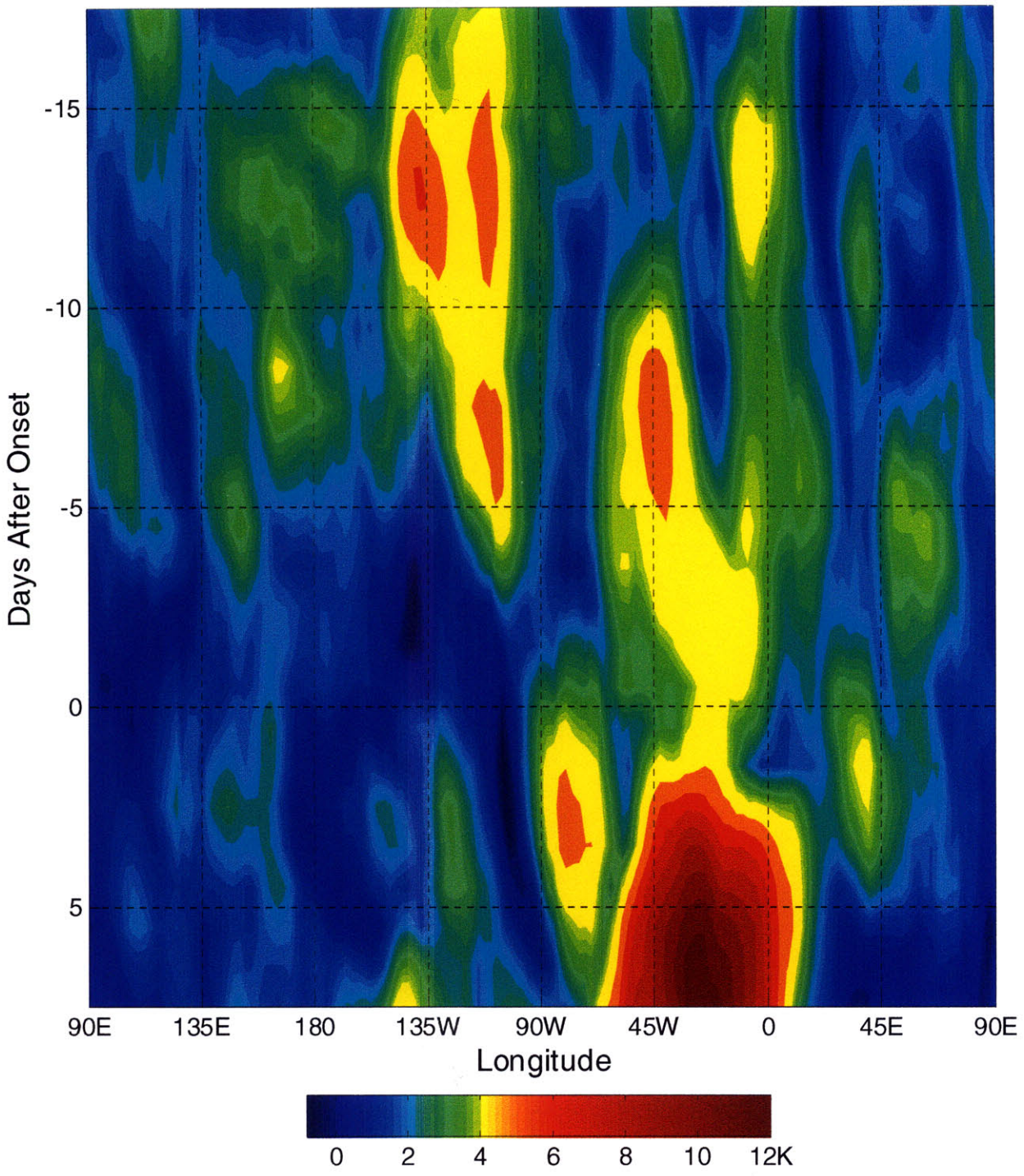

Figure 19: Hovmöller diagram of maximum composite anomalies in a modified blocking index wherein the central blocking latitude varies from 30°N–55°N. An anomalous meridional signal over the eastern Pacific one to two weeks before block onset propagates down to the Atlantic just prior to block onset. Note the cold land detected over North America just prior to block onset that favors the formation of a surface cyclone over the western Atlantic. Contour interval is every 0.2 K from -1 K to 4 K, and 1 K thereafter.

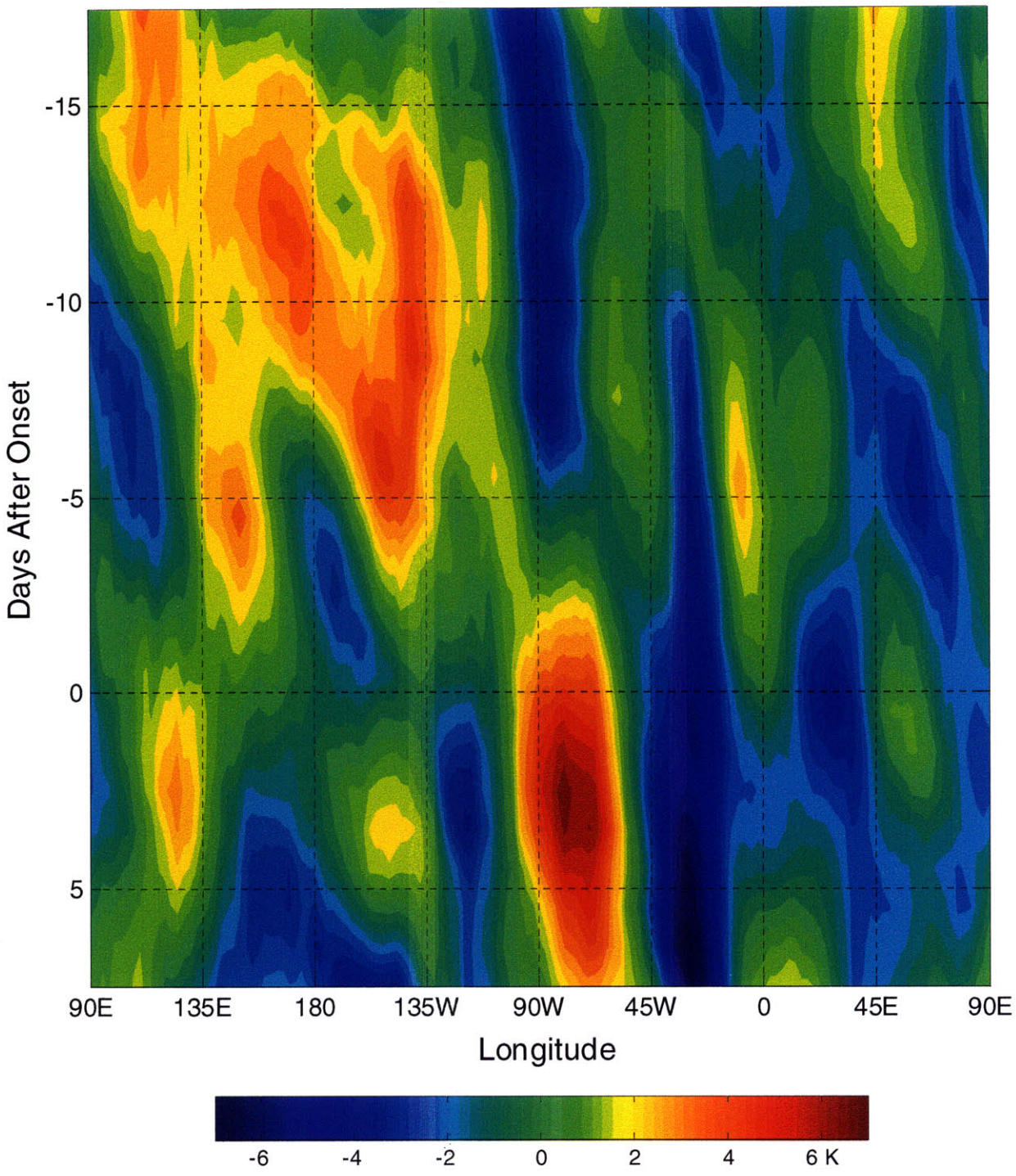

Figure 20: Hovmöller diagram of composite θ_{trop} anomalies averaged between 27.5°N and 37.5°N, showing the precursor signal. Anomalous warm tropopause is advected from the subtropical Pacific down to the Atlantic several days before Atlantic block onset, when strong cyclogenesis also develops over the southeastern United States. Contour interval is 0.5 K.

5.4 Anomalous Meridional Wind — A Consistency Check of the Blocking Signal

A Hovmöller diagram of midlatitude tropopause meridional wind anomalies (Fig. 21) also shows the warm tropopause transport a few days before block onset. The meridional wind diagram illustrates how the anomalous meridional flow established by the PNA+ pattern (more on this in section 6) two weeks prior to block onset persists over both ocean basins, and could contribute to block formation.

Blocking can be thought of as amplifying the climatological meridional flow both upstream and downstream of its center. This aspect of blocking can be clearly seen in the Hovmöller diagram (Fig. 21), where the longitudinal region between approximately 30°W–80°W experiences an anomalous increase. Referring to the V_{trop} climatology (Fig. 8b), the same region also exhibits a maximum on average. This anomalous meridional wind aspect of blocking will be referred to as a blocking 'signal', and can be used to identify Atlantic blocks as part of a consistency check. Are the same blocking events identified using this approach?

To define a blocking event using this signal, 10-day averages of meridional wind anomalies are calculated over the region spanning 40°N–80°N and 30°W–80°W. Values are weighted by the cosine of latitude. Thereafter, a block is defined as occurring if the 10-day averaged anomaly for this region exceeds 5 ms^{-1} (or approximately twice its typical value). Table 2 provides details on the 44 cases identified, and whether or not they are the same as ones found using the Pelly and Hoskins index. 19 of the 32 cases were identified using this method, with most of them lasting much longer than the 10-day minimum blocking duration.

Again, the greatest number of cases occur during the middle of winter (Fig. 22). The most persistent events constitute a large majority of the mid-winter cases, suggesting that large-

scale processes may have considerable influence on persistent anomalous meridional wind (blocking) events.

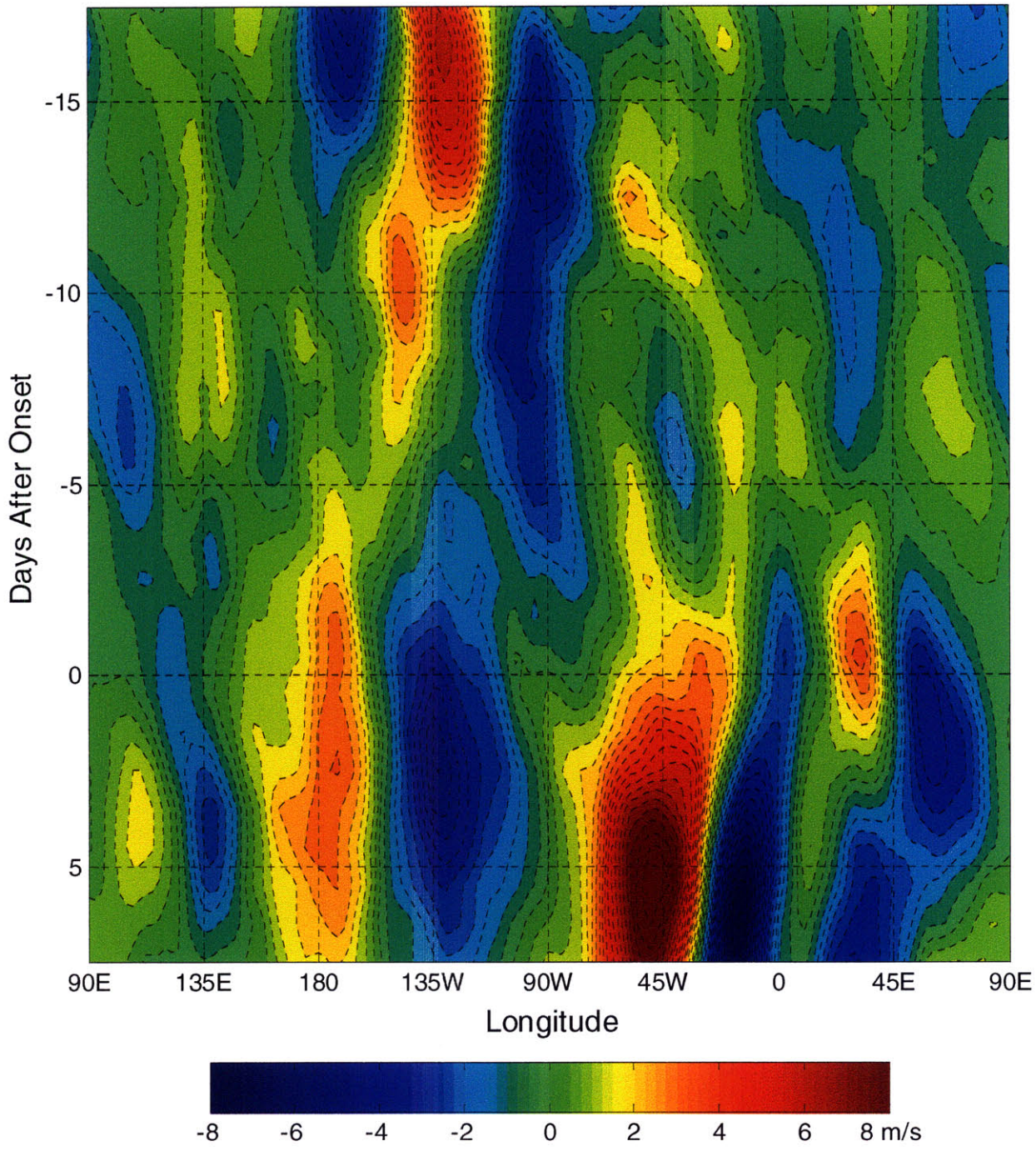

Figure 21: Hovmöller diagram of composite tropopause meridional wind anomalies averaged between 40°N and 70°N, showing the precursor signal. Contour interval is 0.5 ms^{-1}.

Table 2: Anomalous Meridional Wind Events over Atlantic

Case Number	Blocked Period	Block Duration (Days)	Same case as previous?
1	February 15 – 26, 1958	12	no
2	March 20 – 30, 1960	11	yes (case #2)
3	January 23 – February 27, 1962	36	yes (#4)
4	December 7, 1962 – February 5, 1963	61	yes (#5)
5	January 8 – March 6, 1964	59	yes (#7)
6	January 24 – February 28, 1965	36	yes (#8)
7	December 28, 1966 – February 14, 1967	49	yes (#9)
8	December 19, 1967 – January 6, 1968	19	no
9	February 29 – March 15, 1968	16	yes (#10)
10	December 23, 1968 – January 1, 1969	10	no
11	February 18 – March 2, 1970	13	no
12	December 16, 1970 – January 1, 1971	17	yes (#11)
13	December 26, 1971 – January 5, 1972	11	yes (#12)
14	February 15 – March 1, 1972	16	no
15	February 12 – March 2, 1973	19	no
16	December 1 – 22, 1975	22	yes (#16)
17	January 14 – 27, 1976	14	no
18	December 13 – 30, 1976	18	yes (#17)
19	December 21, 1977 – January 6, 1978	17	no
20	January 9 – 21, 1978	13	no
21	January 4 – 16, 1980	13	no
22	February 24 – March 7, 1980	13	no
23	December 29, 1980 – January 17, 1981	20	no
24	February 3 – February 14, 1981	12	no
25	January 29 – February 18, 1983	21	yes (#21)
26	March 21 – 31, 1983	11	no
27	December 28, 1983 – January 14, 1984	18	no
28	February 28 – March 18, 1984	20	yes (#22)
29	January 22 – February 2, 1986	12	yes (#23)
30	January 14 – February 2, 1987	20	yes (#24)
31	February 14 – March 6, 1988	22	no
32	December 3 – 22, 1988	20	no
33	December 1 – 13, 1989	13	yes (#25)
34	January 15 – 31, 1991	17	no
35	February 7 – 21, 1991	15	no
36	January 7 – 24, 1992	18	no
37	March 14 – 29, 1992	16	no
38	February 11 – March 5, 1993	23	yes (#27)
39	December 18, 1993 – January 2, 1994	16	no
40	January 13 – 26, 1994	14	no
41	January 20 – March 11, 1996	52	yes (#28)
42	March 6 – 22, 1998	17	no
43	January 2 – 16, 1999	15	no
44	January 7 – 31, 2000	25	yes (#31)

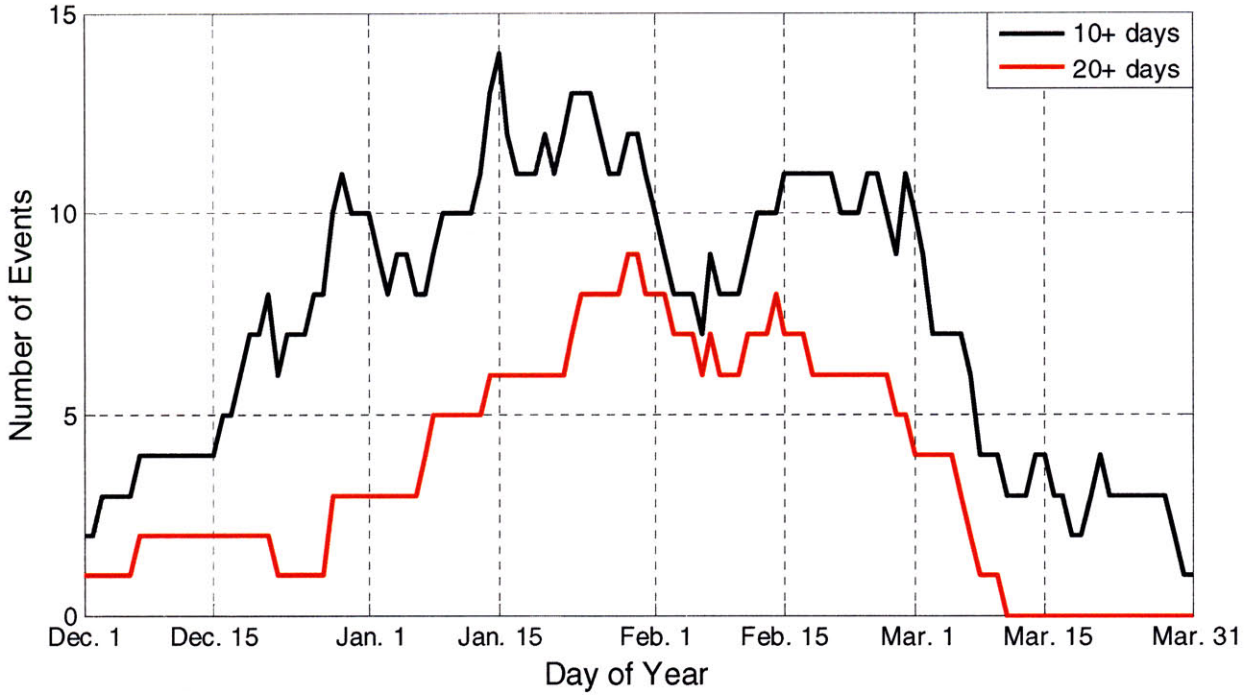

Figure 22: Number of blocking events detected using the meridional wind signal that last at least 10 days (black line) and 20 days (red line). Note the higher frequency and duration of events during the middle of winter.

Out of the 44 Atlantic blocking events identified using the meridional wind signal, 25 were not found using Pelly and Hoskins' index. These cases were examined individually, and most would be considered blocks by a synoptician. However, these cases shared a common blocking center location slightly farther south than the meridional extent used in Pelly and Hoskins' index (see Fig. 23 for a comparison). This finding exemplifies a limitation of Pelly and Hoskins' index that they recognize (Tyrlis and Hoskins 2008a). Since the index does not follow the actual storm track with time, some Rossby wave-breaking events will not be identified.

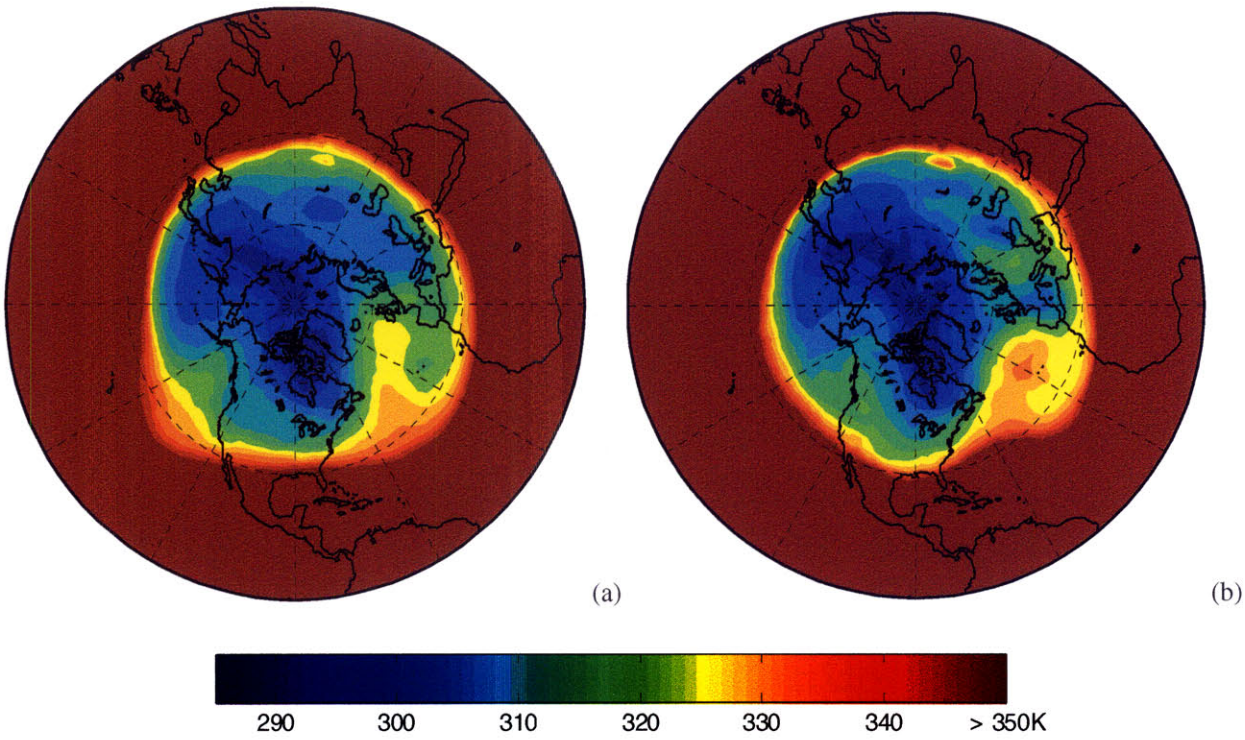

Figure 23: θ_{trop} contoured every 5 K: (a) average of February 1993 case detected using both the blocking index and the meridional wind blocking signal, and (b) January 1978 case detected using the meridional wind signal but not the index because the center of blocking action is shifted slightly south.

Composites of θ_{trop}, U_{trop}, and V_{trop} (Fig. 24) for the 44 cases follow a similar progression to those found using Pelly and Hoskins' index, confirming the "consistency check" that persistent blocking events can also be detected by an anomalously strong and persistent meridional signal.

The composite analysis again confirms the notion that persistent Atlantic blocking events are rooted in global precursors. Redefining what is meant by "persistent" sheds more light on the role of global signals in blocking, and the relationship between large-scale climate modes (teleconnections) and persistent blocking events. Winter season (DJFM) averages of θ_{trop} anomalies reveal that certain years tend to be persistently blocked or close to this state. A composite of thirteen such years over the period of record (Fig. 25) illustrates the preferred climate mode for persistent Atlantic blocking events.

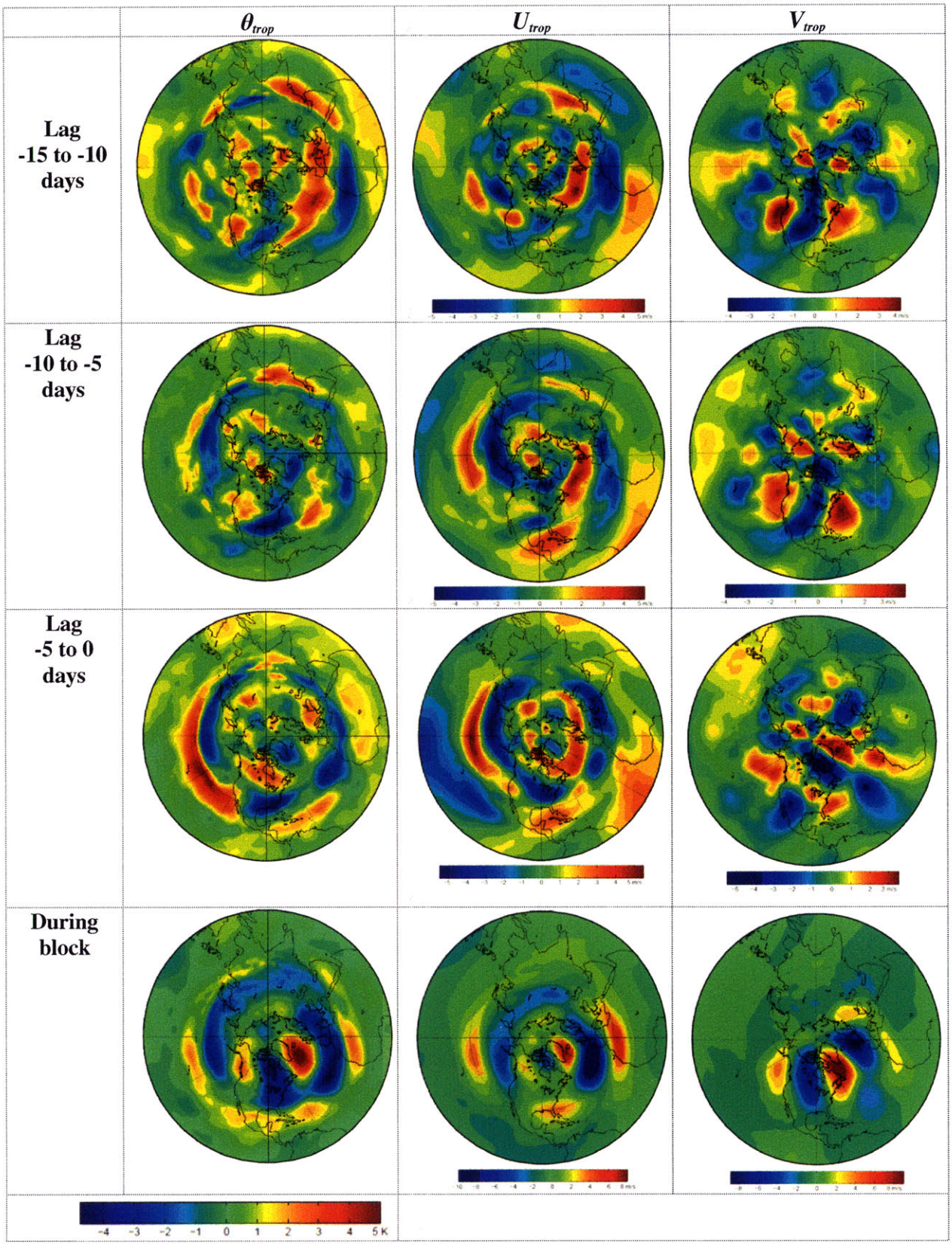

Figure 24: 5-day average composites of θ_{trop}, U_{trop}, and V_{trop} prior to and during the 44 cases identified using the meridional wind blocking signal.

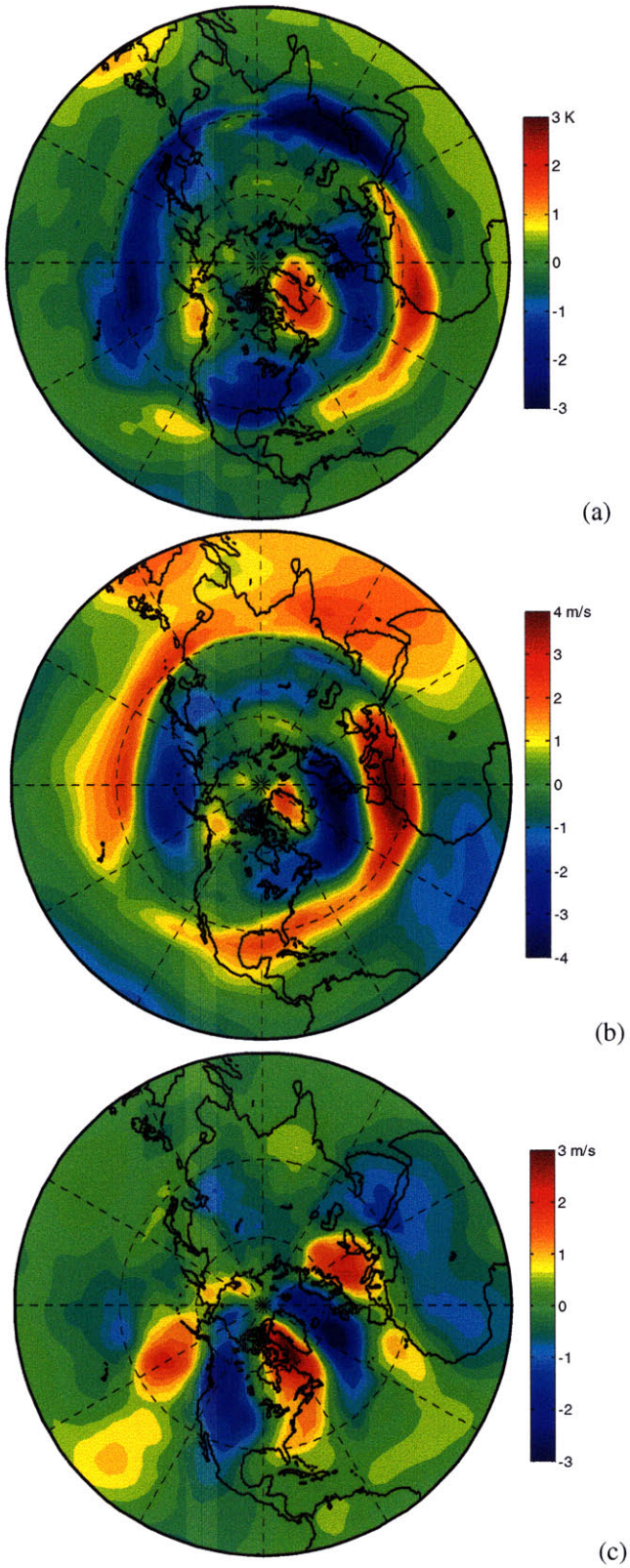

Figure 25: Composite anomalies of (a) θ_{trop}, (b) U_{trop}, and (c) V_{trop} for the thirteen winter seasons closest to an Atlantic blocked state (DJFM 1961/2, 1962/3, 1963/4, 1964/5, 1968/9, 1969/70, 1975/6, 1976/7, 1978/9, 1982/3, 1983/4, 1985/6, and 1995/6).

6 Relationships between Atlantic Blocking and Teleconnections

Teleconnection patterns are related to standing oscillations of planetary waves, and thus are useful to further characterize global precursors to long-lived Atlantic blocking events. Generally, teleconnections are defined as the strongest contemporaneous correlations among either the sea level pressure or 500 hPa height fields (Wallace and Gutzler 1981). This analysis used a database of daily teleconnection indices for the time period December 1957 to March 2002 (NWS-CPC 2005a). An explanation for how the daily indices are calculated is located on the web site of the National Weather Service (NWS-CPC 2005b).

The three main Northern Hemisphere teleconnections are considered here: the Pacific/North American pattern (PNA), the North Atlantic Oscillation (NAO), and the Arctic Oscillation (AO). Figure 26 provides schematics of θ_{trop} anomalies for one phase of each index.

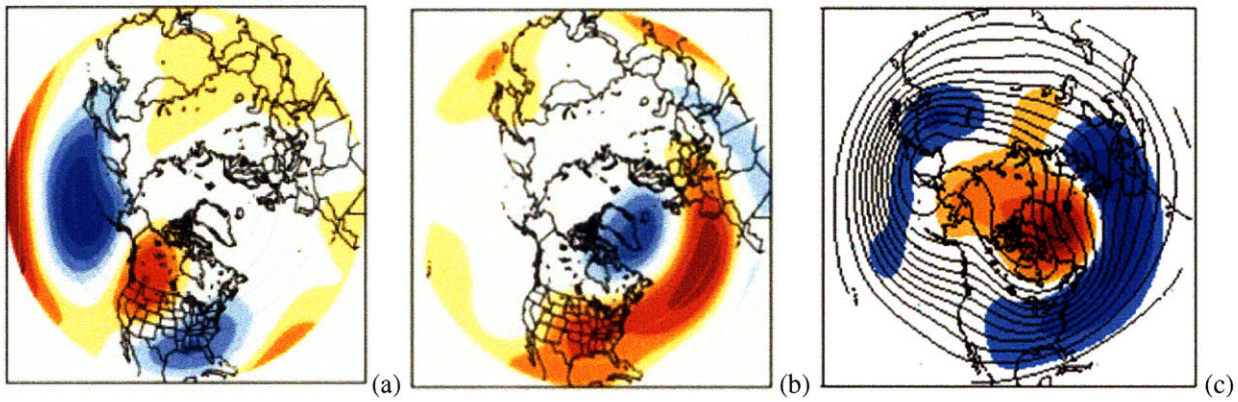

Figure 26: Winter positive phase of the (a) PNA and (b) NAO, and the (c) negative phase of the AO, with red (blue) shading indicating regions of anomalously warm (cold) tropopause. Images taken from the Climate Prediction Center web site.[1]

[1] (PNA image) http://www.cpc.ncep.noaa.gov/data/teledoc/pna_map.shtml;
(NAO image) http://www.cpc.ncep.noaa.gov/data/teledoc/nao_map.shtml;
(AO image) http://www.cpc.ncep.noaa.gov/research_papers/ncep_cpc_atlas/8/figures/z500/JFM.z500.ao.gif

As shown in Fig. 26, the PNA is comprised of four centers. Two upstream anomaly centers are located near Hawaii and the North Pacific, while the downstream anomaly centers are located over Alberta and the southeastern United States. The PNA+ phase is characterized by a deep Aleutian low and ridging over Alberta. As mentioned in section 5, the Pacific precursor signal established two weeks prior to block onset resembles the PNA+ phase. A composite time series of the PNA index for cases identified using the Pelly and Hoskins index does indeed show a significant PNA+ phase two weeks prior to block onset (Fig. 27). Recently, it has been shown that the PNA+ positive phase can be triggered by anomalous tropical convection over the western Pacific (Franzke et al. 2007).

The NAO is the leading variability pattern during Northern Hemisphere winter, (Barriopedro et al. 2006), and consists of anomaly centers over the central Atlantic and Greenland. The literature also shows that blocking preferentially associates with the NAO- phase (Croci-Maspoli et al. 2007b, Benedict et al. 2008). The composite time series of the NAO index (Fig. 27) shows that a significant NAO+ phase (typically a strong zonal Atlantic jet) transitions to the NAO- phase during the mature phase of Atlantic blocking.

Thompson and Wallace (1998, 2000), and Wallace (2000) have demonstrated that a third teleconnection pattern, the AO, plays an important role in mechanisms responsible for Northern Hemisphere variability. The AO is associated with two anomaly centers: one over the polar region, and another of opposite sign distributed over the midlatitudes. The NAO and AO are highly correlated, but the NAO lacks a center of action over the Pacific. Thompson and Wallace (2000) proposed that the AO may the manifestation of a zonally symmetric mode — the so-called "annular mode" — altered by topography and other zonally asymmetric forcings. The composite AO time series in Fig. 27 demonstrates that the AO trends significantly negative

immediately before and during Atlantic blocking, suggesting a global signature associated with the persistent blocking events. Also note in Fig. 27 that the AO decline leads the NAO drop by several days, signifying the important role of global processes in establishing the Atlantic block.

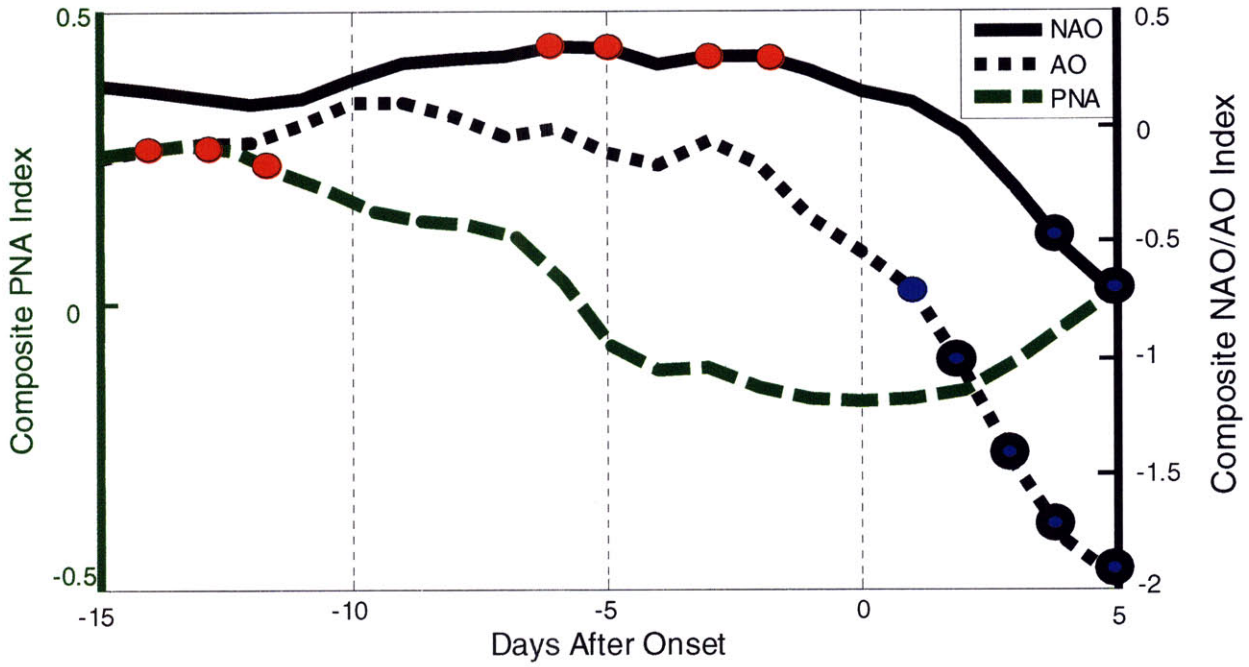

Figure 27: Time series of composite teleconnection indices for persistent Atlantic blocking events. The left (right) vertical axis provides the scale for the composite PNA (NAO and AO) index. Days during which the composite indices are significantly positive (negative) are depicted with red (blue) dots. (Un)bolded dots indicate significance at the (95) 99% confidence level using a one-tailed Student's t test.

Teleconnections can also help explain the observation from section 5 of a trend toward fewer persistent Atlantic blocking events over the period of record. The NAO index, an indicator of Atlantic blocking, trended positive over the ERA-40 period of record. The trend is consistent with the observed decreasing blocking frequency. Computing Pearson correlation coefficients for linear trends in θ_{trop} across the Northern Hemisphere illustrates the NAO trend (Fig. 28). High latitudes over the Atlantic experienced a decrease in θ_{trop}, while the opposite trend occurred over the midlatitudes, suggesting that either blocking frequency and/or duration have decreased over the last half century, or perhaps that the mean location of the storm track

shifted south during the period and now blocking occurs more frequently farther south. These results are consistent with a similar analysis undertaken by Woollings et al. (2008).

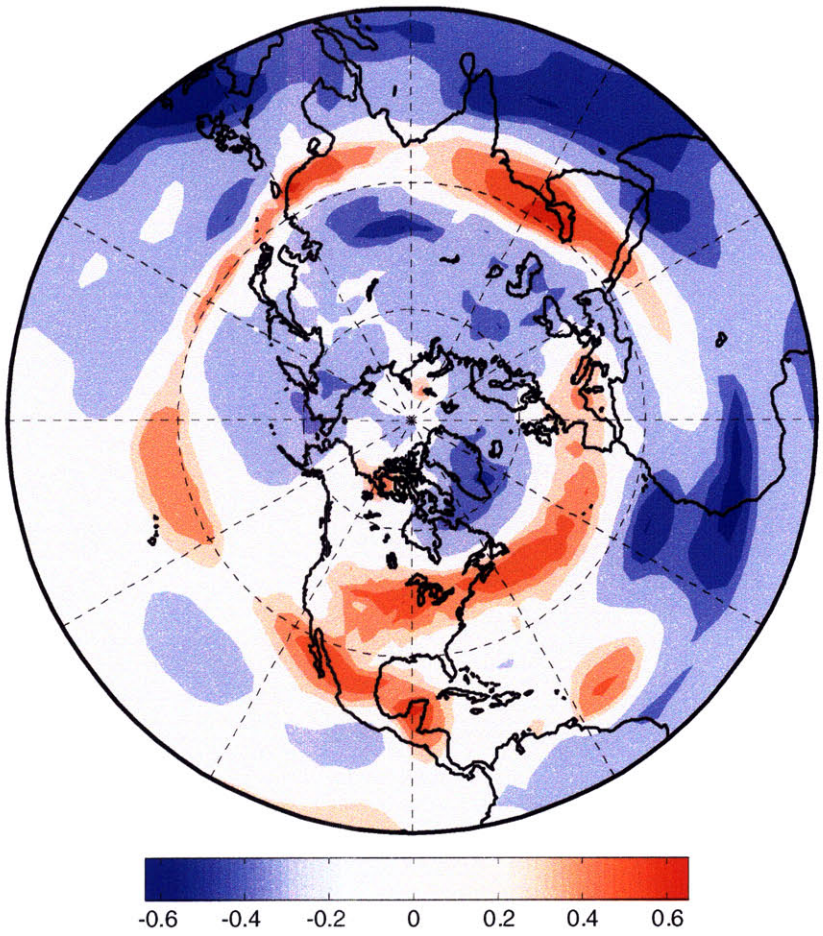

Figure 28: Correlation coefficient of linear trends in θ_{trop} (DJFM 1957/8 – 2001/2). Contour interval is 0.1, with non-significant values ($p > 0.05$) between -0.3 and 0.3 shaded white. Areas shaded red (blue) experienced a significant increase (decrease) in θ_{trop} over the period of record.

7 Summary of Findings

This work has described conditions along the dynamical tropopause conducive for development of persistent Atlantic blocking events. A composite analysis and Hovmöller diagrams clearly identify several dynamical precursors to these blocking events. Results suggest that the PNA+ pattern occurring one–two weeks prior to block onset establishes an enhanced meridional signal over the Atlantic. As the PNA transitions to its negative phase, an anomalous cold tropopause over western North America spurs cyclogenesis downstream over the southeastern United States. Atlantic cyclones then interact with the enhanced meridional signal previously established over the Atlantic, stretch meridionally, and promote blocking genesis and maintenance.

Recently, it has been shown that the PNA+ positive phase can be triggered by anomalous tropical convection over the western Pacific (Franzke et al. 2007). Understanding the processes triggering the anomalous tropical activity, and other PNA+ precursors, would provide a more complete description of the Atlantic blocking precursor signal found here.

The mature phase of Atlantic blocking strongly resembles the negative phases of other main modes of atmospheric variability, namely the NAO and AO, consistent with prior studies (Croci-Maspoli et al. 2007b, Woollings et al. 2008). The association of Atlantic blocking to simultaneous changes of multiple large-scale climate modes further suggests that persistent blocking events are a global, rather than localized, phenomenon.

Further insight might be gained into blocking precursors by exploring the state of the stratosphere prior to block onset. Many researchers have looked at how troposphere blocking affects the stratosphere, but the opposite perspective is less frequently considered. Vertically-propagating waves exchanged between the stratosphere and troposphere have been well-

documented, and can induce changes in one or both layers. The statistical study of Taguchi (2008) found no significant association between sudden stratospheric warmings and blocking as indicated by the 500 hPa height field, but others have found small, yet significant, correlations between the state of the polar vortex and blocking using θ_{trop} as the blocking indicator (Woollings et al. 2008).

8 References

Barriopedro, D., et al., 2006: A climatology of Northern Hemisphere blocking. *J. Climate*, **19**, 1042–1063.

Benedict, J. J., S. Lee, and S. B. Feldstein, 2004: Synoptic view of the North Atlantic Oscillation. *J. Atmos. Sci.*, **61**, 121–144.

Berrisford, P., B. J. Hoskins, and E. Tyrlis., 2007: Blocking and Rossby wave breaking on the dynamical tropopause in the Southern Hemisphere. *J. Atmos. Sci.*, **64**, 2881–2898.

Croci-Maspoli, M., C. Schwierz, and H. C. Davies, 2007a: A multifaceted climatology of atmospheric blocking and its recent linear trend. *J. Climate*, **20**, 633–649.

——, ——, and ——, 2007b: Atmospheric blocking: space-time links to NAO and PNA. *Clim. Dyn.*, **29**, 713–725.

Franzke, C., S. B. Feldstein, and S. Lee, 2007: Synoptic analysis of the Pacific-North American teleconnection pattern. AGU Fall meeting, abstract A13E-1612.

Hansen, A. R., and A. Sutera, 1993: A comparison between planetary-wave flow regimes and blocking. *Tellus*, **45A**, 281–288.

Hoskins, B. J., M. E. McIntyre, and A. W. Robertson, 1985: On the use and significance of isentropic potential vorticity maps. *J. Meteor. Soc. Japan*, **79**, 877–946.

Martius, O., C. Schwierz, and M. Sprenger, 2008: Dynamical tropopause variability and potential vorticity streamers in the Northern Hemisphere – a climatological analysis. *Adv. in Atmos. Sci.*, **25**, 367–379.

National Center for Atmospheric Research (NCAR): The ERA-40 archive at NCAR. 19 May 2009, http://dss.ucar.edu/pub/era40/.

National Weather Service – Climate Prediction Center, 2005a: Teleconnections: archive of daily indices. 19 May 2009, ftp://ftp.cpc.ncep.noaa.gov/cwlinks.

——, 2005b: Teleconnection pattern calculation procedures. 19 May 2009, http://www.cpc.ncep.noaa.gov/data/teledoc/telecontents.shtml.

Pelly, J. L., and B. J. Hoskins, 2003: A new perspective on blocking. *J. Atm. Sci.*, **60**, 743–755.

Rex, D. F., 1950a: Blocking action in the middle troposphere and its effect upon regional climate. I. An aerological study of blocking action. *Tellus*, **2**, 196–211.

——, 1950b: Blocking action in the middle troposphere and its effect upon regional climate. II. The climatology of blocking action. *Tellus*, **2**, 275–301.

Taguchi, M., 2008: Is there a statistical connection between stratospheric sudden warming and tropospheric blocking events? *J. Atm. Sci.*, **65**, 1442–1454.

Thompson, D. W. J., and J. M. Wallace, 1998: The arctic oscillation signature in wintertime geopotential height and temperature fields. *Geophys. Res. Lett.*, **25**, 1297–1300.

——, and ——, 2000: Annular modes in the extratropical circulation. Part I: Month-to-month variability. *J. Climate*, **13**, 1000–1016.

Tibaldi, S., and F. Molteni, 1990: On the operational predictability of blocking. *Tellus*, **42A**, 343–365.

Tyrlis, E., and B. J. Hoskins, 2008a: Aspects of a Northern Hemisphere blocking climatology. *J. Atmos. Sci*, **65**, 1638–1652.

——, and ——, 2008b: The morphology of Northern Hemisphere blocking. *J. Atmos. Sci*, **65**, 1653–1665.

Uppala, S. M., et al., 2005: The ERA-40 re-analysis. *Quart. J. Roy. Meteor. Soc.*, **131**, 2961–3012.

Wallace, J. M., and D. S. Gutzler, 1981: Teleconnections in the geopotential height field during the Northern Hemisphere winter. *Mon. Wea. Rev.*, **109**, 784–812.

——, 2000: North Atlantic Oscillation/annular mode: Two paradigms – one phenomenon. *Q. J. R. Meteorol. Soc.*, **126**, 791–805.

Woollings, T., et al., 2008: A new Rossby wave-breaking interpretation of the North Atlantic Oscillation. *J. Atmos. Sci.*, **65**, 609–626.

Appendix: Complete evolution of composite tropopause θ, U, and V anomalies for the Atlantic block cases

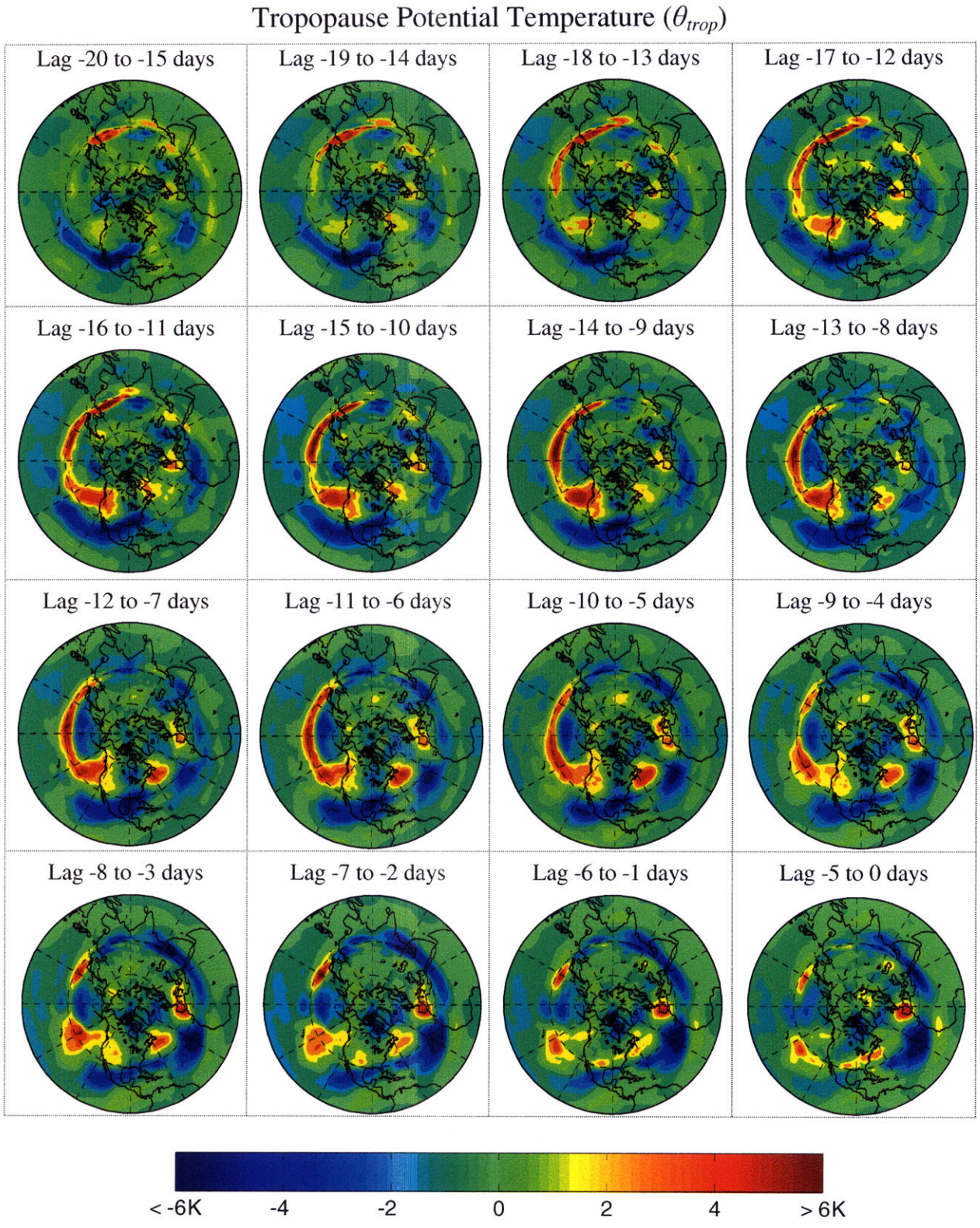

θ_{trop}, continued

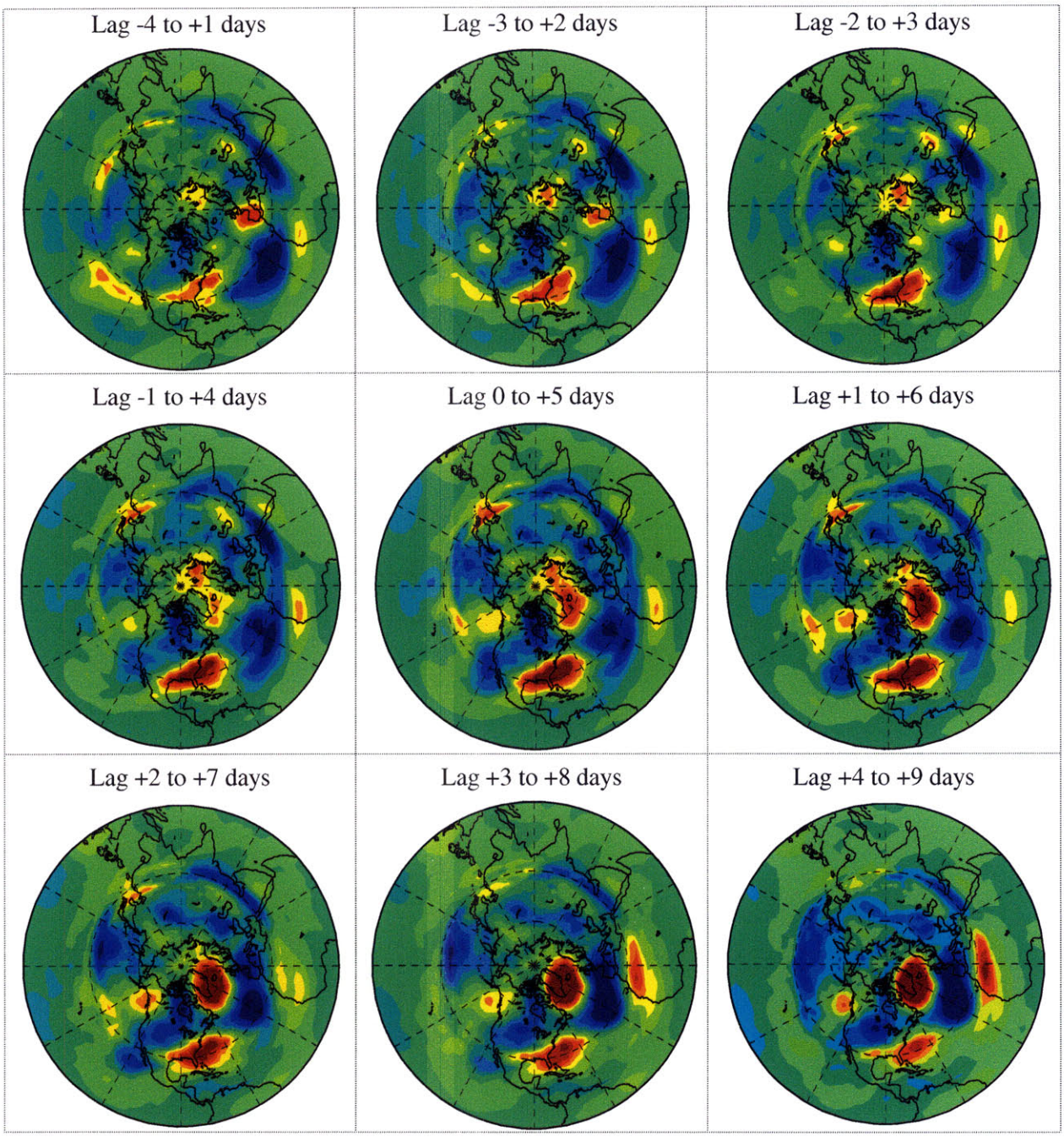

Tropopause Zonal Wind (U_{trop})

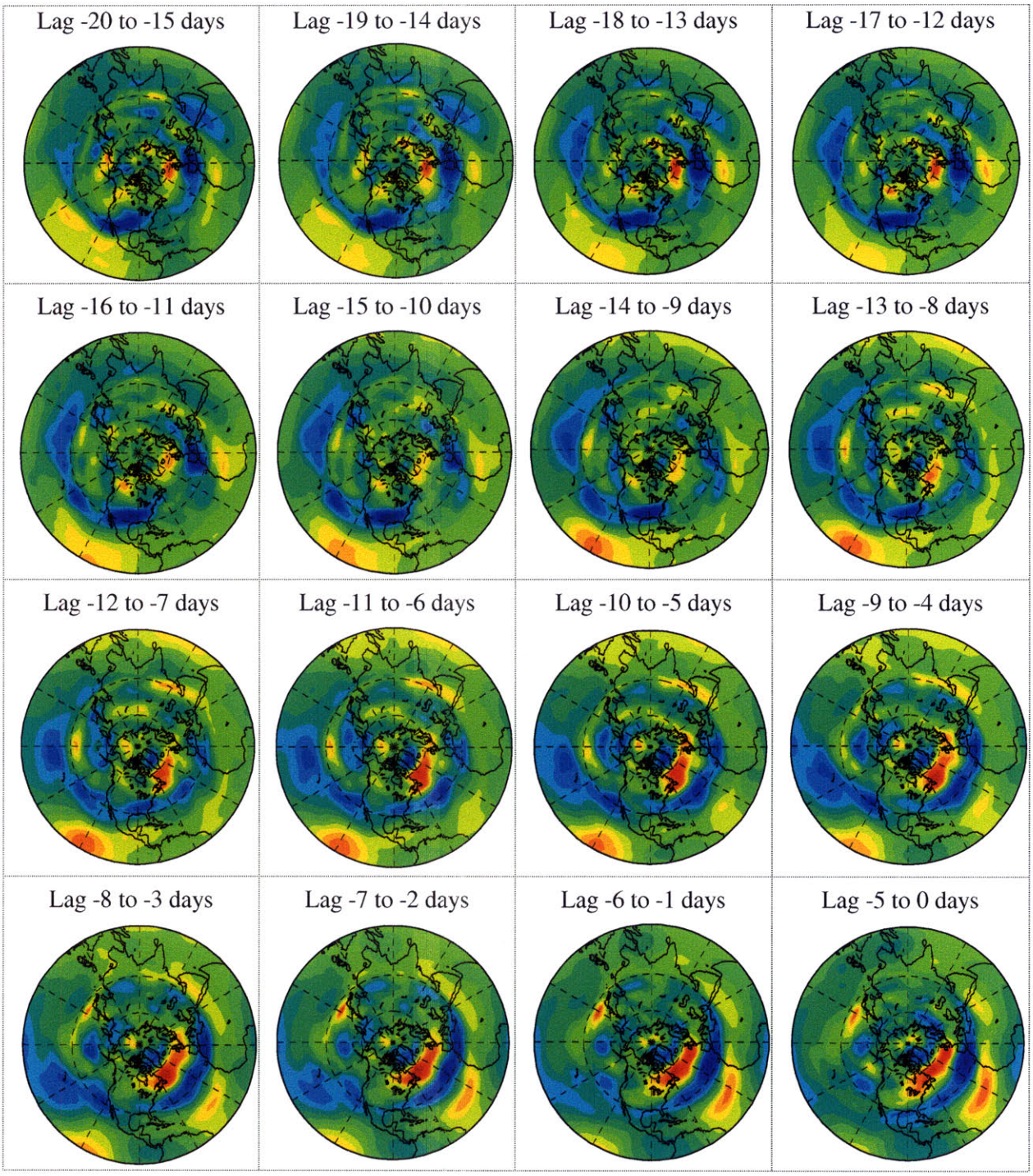

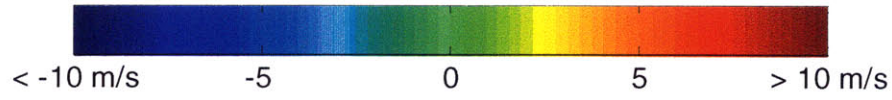

U_{trop}, continued

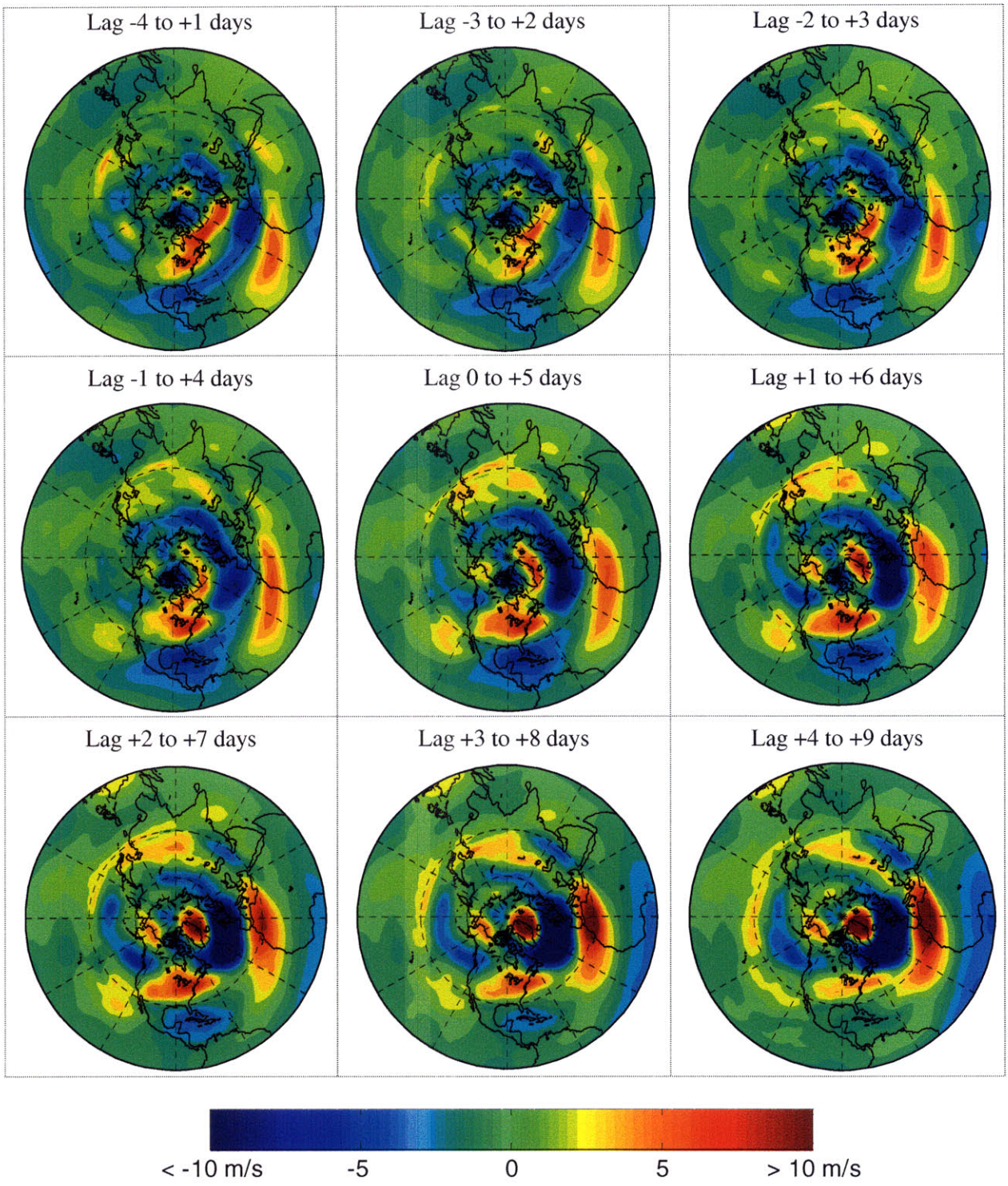

Tropopause Meridional Wind (V_{trop})

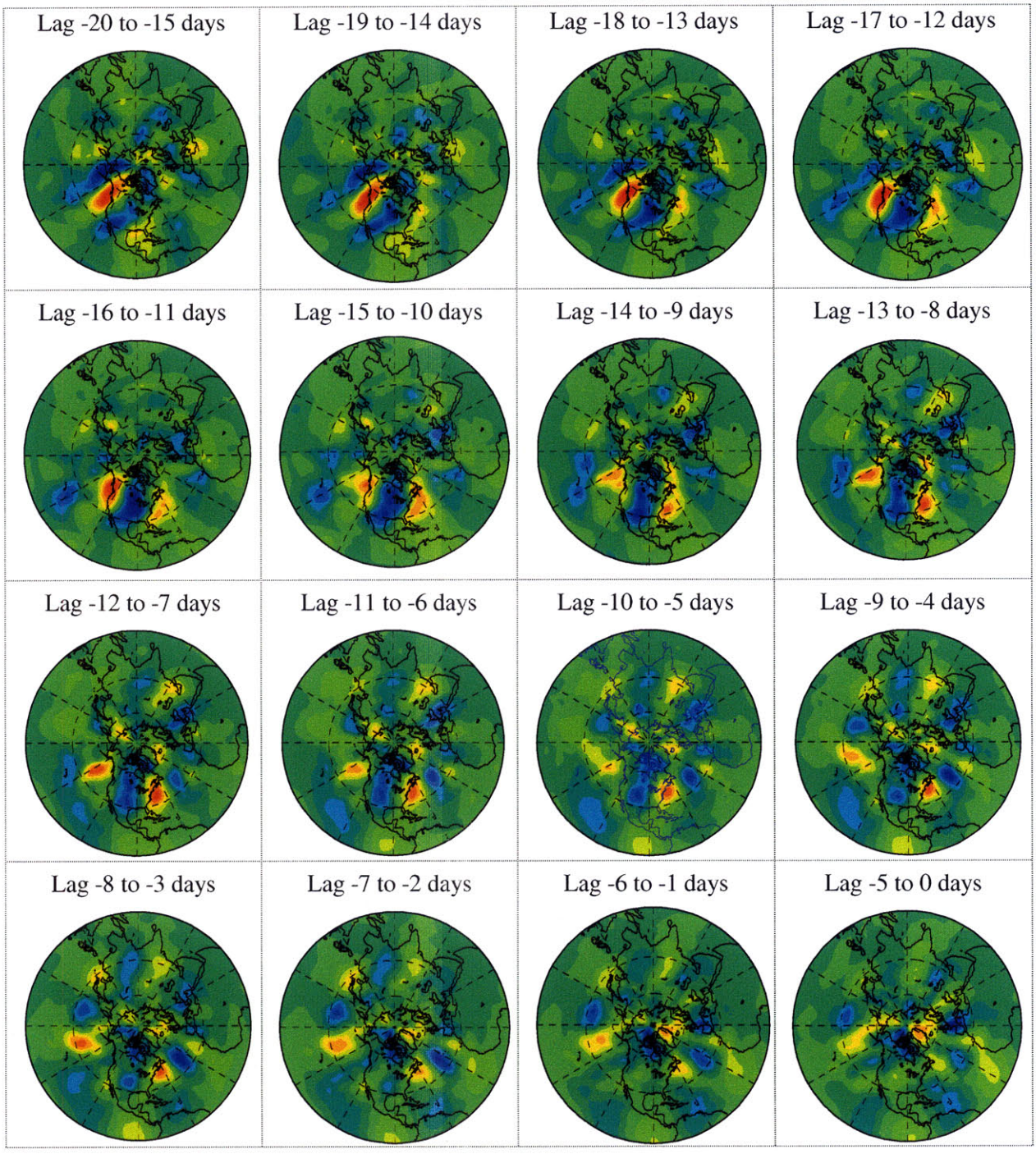

V_{trop}, continued